CR 134514

DEVELOPMENT OF HIGH-EMITTANCE SCALES ON THORIATED NICKEL-CHROMIUM-ALUMINUM-BASE ALLOYS

to

NATIONAL AERONAUTICS AND SPACE ADMINISTRATION
Technical Management
NASA-Lewis Research Center
Cleveland, Ohio

Contract NAS3-15845

October 15, 1973

by

M. S. Seltzer, I. G. Wright, and B. A. Wilcox

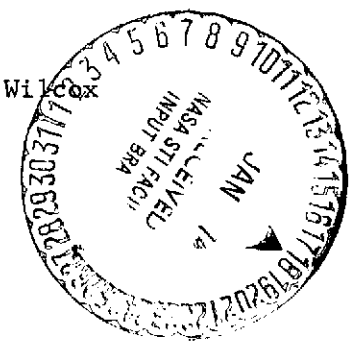

BATTELLE
Columbus Laboratories
505 King Avenue
Columbus, Ohio 43201

1. Report No.	2. Government Accession No.	3. Recipient's Catalog No.
CR 134514		

4. Title and Subtitle	5. Report Date
Development of High-Emittance Scales on Thoriated Nickel-Chromium-Aluminum-Base Alloys	October 15, 1973
	6. Performing Organization Code
7. Author(s)	8. Performing Organization Report No.
M.S. Seltzer, I.G. Wright, and B. A. Wilcox	
9. Performing Organization Name and Address	10. Work Unit No.
Battelle - Columbus Laboratories 505 King Avenue Columbus, Ohio 43201	11. Contract or Grant No. NAS3-15845
12. Sponsoring Agency Name and Address	13. Type of Report and Period Covered Contractor Report, July 1, 1972 to Aug. 31, 1973
National Aeronautics & Space Administration Washington, D.C. 20546	14. Sponsoring Agency Code

15. Supplementary Notes

Project Manager, Dr. Gilbert Santoro, Materials and Structures Division, NASA-Lewis Research Center, Cleveland, Ohio

16. Abstract

The surface regions of a DSNiCrAl alloy have been doped, by a pack diffusion process, with small amounts of Mn, Fe, or Co, and the effect of these dopants on the total normal emissivity of the scales produced by subsequent high-temperature oxidation has been measured. While all three elements lead to a modest increase in emissivity, (up to 23% greater than the undoped alloy) only the change caused by manganese is thermally stable. However, this increased emissivity is within 85 percent of that of TDNiCr oxidized to form a chromia scale. The maganese-doped alloy is some 50 percent weaker than undoped DSNiCrAl after the doping treatment, and approximately 30 percent weaker after oxidation.

17. Key Words (Suggested by Author(s))	18. Distribution Statement
Emittance of alumina scales Oxidation Doped DSNiCrAl	Unclassified-Unlimited

19. Security Classif. (of this report)	20. Security Classif. (of this page)	21. No. of Pages	22. Price*
Unclassified	Unclassified		$3.00

* For sale by the National Technical Information Service, Springfield, Virginia 22151

TABLE OF CONTENTS

LIST OF FIGURES

LIST OF FIGURES - Continued

LIST OF TABLES

FOREWORD

This report was prepared by the personnel of Battelle-Columbus, Columbus, Ohio, and describes original work performed under Contract NAS3-15845.

The contract was awarded to Battelle-Columbus by the NASA-Lewis Research Center. Technical monitoring was provided by the Project Manager, Dr. G. Santoro, of the Materials and Structures Division of the NASA-Lewis Research Center.

M. S. Seltzer of Battelle-Columbus served as Principal Investigator.

The authors wish to acknowledge helpful discussions with Professor R. A. Rapp of The Ohio State University throughout the course of this program. Thanks are also due to Battelle's Columbus Laboratories for sharing a portion of the cost of this study.

The contract work was performed over the period from July 1, 1972, to August 31, 1973.

DEVELOPMENT OF HIGH-EMITTANCE SCALES ON THORIATED NICKEL-CHROMIUM-ALUMINUM-BASE ALLOYS

by

M. S. Seltzer, I. G. Wright, and B. A. Wilcox

ABSTRACT

The surface regions of a DSNiCrAl alloy have been doped, by a pack diffusion process, with small amounts of Mn, Fe, or Co, and the effect of these dopants on the total normal emissivity of the scales produced by subsequent high-temperature oxidation has been measured. While all three elements lead to a modest increase in emissivity (up to 23% greater than the undoped alloy) only the change caused by manganese is thermally stable. However, this increased emissivity is within 85 percent of that of TDNiCr oxidized to form a chromia scale. The manganese-doped alloy is some 50 percent weaker than undoped DSNiCrAl after the doping treatment, and approximately 30 percent weaker after oxidation.

SUMMARY

The objectives of this program were: (1) to increase the emittance of the alumina scales formed during high-temperature oxidation of Sherritt-Gordon DSNiCrAl alloys; (2) to evaluate the thermal stability of the emittance improvement; and (3) to determine the effect that the doping treatments, which have provided the emittance improvement, have upon the oxidation resistance and the tensile properties of the alloys.

The elements Mn, Fe, and Co were chosen as dopants. Coupons of the as-received alloy and coupons which had been preoxidized were pack-annealed in mixtures of 83% alumina powder, 1% sodium chloride, 1% urea, and 15% of a Ni-Cr-Al alloy containing 5% Mn, Fe, or Co, in an attempt to introduce small amounts of the dopants into the surfaces of the alloys or directly into the preformed scales. Deposition of a thin layer of alloy on the surface of the specimens, and doubts about the stability of the preformed oxide scale in the pack led to the abandonment of attempts to dope alumina scales directly.

The doped alloys were exposed to isothermal and cyclic oxidation tests at 1373 and 1473°K (1100 and 1200°C) in slowly-flowing air at 1.33×10^3 and 1.01×10^5 N/m^2 (10 and 760 torr) for 1.8×10^5 s (50 h), and emittance measurements of the scales formed were made to rank the effectiveness of the dopants. All three doped alloys gave emittances some 17 to 23% greater than that of the undoped alloy, but only the emittance improvement caused by the manganese addition proved thermally stable.

Subsequent examination of the oxidation behavior of the DSNiCrAl-Mn alloy revealed that its oxidation kinetics were almost identical to those of the undoped alloy. An outer layer of brown-colored, $MnAl_2O_4$-containing oxide formed on the doped alloy, and the presence of a manganese concentration gradient in the main alumina scale was detected, but apparently has virtually no effect on the oxidation rate.

The manganese-doped alloy was approximately 50% weaker and less ductile than the as-received alloy after the pack diffusion process, which may have been related to the formation of a hard, aluminum-enriched surface layer. After oxidation, when the dopant concentration gradients of elements introduced from the pack were flattened, the doped alloy was still 30% weaker, and less ductile than the undoped, oxidized alloy. The increased aluminum content, to approximately 9%, resulting from the pack treatment, may have been responsible for this change.

I. INTRODUCTION

Among the possible materials for use in the outer skin or thermal protection system (TPS) of reusable space vehicles are various thoriated nickel-chromium-base alloys. Initial experiments[1] in static air suggested that these alloys would exhibit excellent oxidation resistance and relatively high strength at the temperatures of interest (1273-1473°K (1000-1200°C)). Later tests in arc-jet facilities [2-4], involving high flow rates, revealed serious weight loss and depletion of chromium from these alloys, as the result of rapid volatilization of the protective Cr_2O_3 oxide scale as CrO_3. It therefore became apparent that in order to utilize thoriated nickel-chromium-base alloys for multiple reentries under conditions where skin temperatures approach 1473°K (1200°C), it would be desirable to improve the oxidation resistance of these alloys.

One approach which has been taken to solve this problem is to add sufficient aluminum to the alloys to produce a protective, non-volatile Al_2O_3 scale upon oxidation. This has been accomplished either by adding aluminum to the alloys during production, or by enriching only the near-surface region by a pack aluminizing process[5]. Both techniques yield alloys which produce light-grey Al_2O_3 scales when oxidized in air in the range of 1273-1473°K (1000-1200°C).

While these thin, adherent scales provide satisfactory protection to the alloys against environmental degradation, they do not satisfactorily meet another requirement for an adequate TPS material, which is the need to maintain a stable high emittance during service life. This is important since radiation cooling is utilized to accommodate the convective heating which occurs during reentry. Centolanzi[2] has measured the surface emissivity for samples of Fansteel alloys, TD-NiCr and TD-NiCrAlY at 1473°K (1200°C) and has found the values to be 0.85 and 0.70 respectively. This difference, which, it is suggested, results from different oxides being formed at the surface during test exposures, could result in a significantly higher radiative equilibrium temperature for the TD-NiCrAlY as compared with TD-NiCr, and diminish the usefulness of alumina-forming thoriated nickel-base alloys as TPS materials. Therefore, in addition to satisfactory oxidation resistance and mechanical properties, it is desired to develop a material with the highest possible emissivity.

The basic concept employed to meet these objectives was that a significant measurable increase in the high-temperature emittance of scales formed on a thoriated NiCrAl alloy could be obtained by doping the scales with foreign atoms which darken the normally light grey Al_2O_3 scales. Small additions of cobalt to alumina are known to have a large effect on the emissivity, for instance an addition of 0.5% Co to Coors AD-96 alumina increases the total emissivity at 1200°C from 0.40 to 0.70[6], and an addition of 2.5% max. Mn is commonly made to Nichrome to improve the emissivity of heating coils.

Two methods were used in an attempt to introduce foreign atoms (Mn, Fe, or Co) to the Al_2O_3 scales. In the first, a pack process was utilized to diffuse dopants into the near-surface region of the alloys, from which they could be rediffused into the scale, produced as the alloy was oxidized at elevated temperatures. The second method involved the direct diffusion-doping of Al_2O_3 scales produced during the controlled oxidation of thoriated NiCrAl alloys.

The effectiveness of the dopants in increasing the emittance was established by direct emittance measurements at 1373 and 1473°K (1100 and 1200°C). The thermal stability of the high emittance scales was determined by a series of isothermal and cyclic oxidation tests conducted at 1373 and 1473°K (1100 and 1200°C) for varying times up to 1.8×10^5 s (50 h). These tests were followed by emittance measurements as well as characterization of the scales by determination of weight change, thickness change, and by various techniques including ion-probe microanalysis.

The room temperature tensile properties of the alloys studied in this program were also evaluated before and after doping and oxidation to pinpoint improvements or degradation of mechanical properties, and therefore fabricability of these potential TPS materials. In order to provide standards for the testing and measurements to be performed on doped alloys, the same tests and measurements were conducted on the as-received alloys.

II. SCREENING TESTS

Characterization of DSNiCrAl

Two square feet of DSNiCrAl sheet (No. 4-1) manufactured by Sherritt-Gordon Mines, Ltd., were supplied by NASA-Lewis Research Center. The nominal thickness of the sheet was 2.54×10^{-4} m (0.0100 in), and the variation in thickness was 2.18×10^{4} to 2.74×10^{-4} m (0.0086 to 0.0108 in); coupons for doping and oxidation tests were taken from an area having a thickness of 2.36×10^{-4} m (0.0093 in). The supplied sheet had a coarse (approximately 100 grit) sanded surface finish, and both sides were found to contain surface defects in the form of holes or craters of diameters up to 1.5 to 2.5×10^{-4} m (0.006 to 0.010 in), which occurred at a frequency of up to 15,500 per square meter.

A typical cross-sectional view of the unetched sheet is shown in Figure 1a, and illustrates the string of porosity which was found in specimens taken from the whole width of the sheet, and which occurred only on one

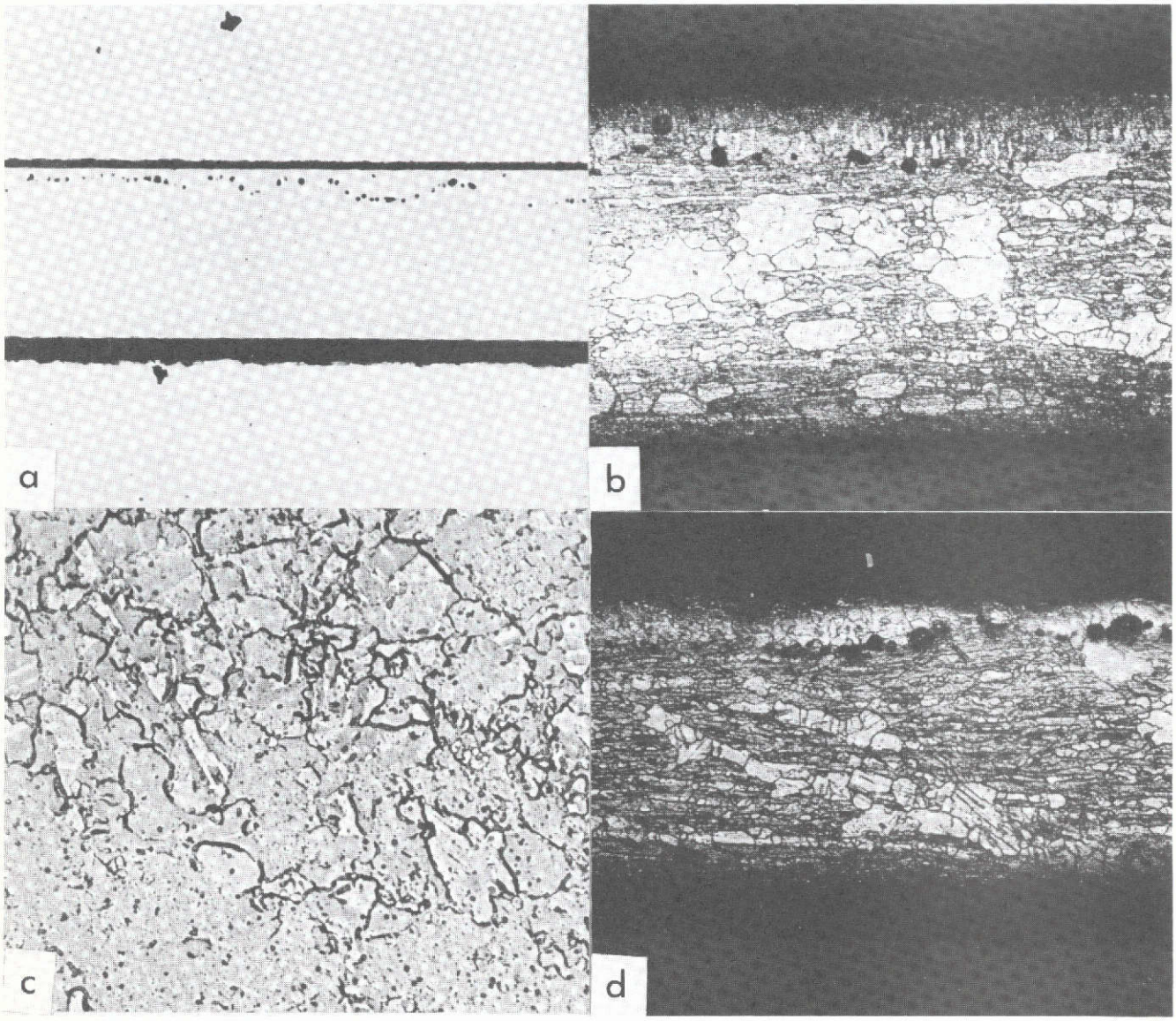

FIGURE 1. MICROSTRUCTURE OF THE AS-RECEIVED DS NiCrAl SHEET

(a) Unetched section normal to the rolling direction, showing a typical string of porosity near one surface, X100.
(b) Etched section normal to the rolling direction, showing the inhomogeneous partially-recrystallized structure, X200.
(c) Surface of the sheet, etched, X200.
(d) Etched section parallel to the rolling direction, X200.

side of the sheet. Three complementary, etched sectional views of the sheet are shown in Figures 1b, 1c, and 1d. The alloy structure is clearly not homogeneous and consists of a partially recrystallized mixture of large, almost equiaxed and often twinned grains (light-etching phase) and elongated, smaller grains. Near the surface, and especially near the string of pores, the grain structure attains a more uniform size (Figure 1d).

Chemical analysis showed the as-received material to be slightly lower in chromium and higher in aluminum than the nominal composition:

	% Ni	% Cr	% Al	% ThO_2	% Mn	% Co	% Fe
Nominal analysis	Bal	14.0-18.0	3.5-5.5	1.60-2.40	-	-	-
Chemical analysis	Bal	13.5	5.9	1.9	0.05	0.04	0.10

but electron-probe microanalysis indicated the alloy was chemically homogeneous.

Pack-Doping of DSNiCrAl

A series of master alloys was prepared for use in the pack diffusion process. The desired alloy compositions (in weight percent) were: (1) Ni-15 Cr-15Al-5Fe, (2) Ni-15Cr-15Al-5Mn, and (3) Ni-15Cr-15Al-5Co. Chemical analyses of the major elemental materials used in preparing the charges for arc melting are given in Table 1. Charges of 0.400 kg total weight were prepared from the above materials and melted in an inert-electrode, copper-crucible, arc furnace. Each charge was melted twice under argon with individual melting time per cycle ranging between 240 and 300 seconds at maximum current of 1400 amperes. No difficulties were encountered in the melting operations. Weight changes during melting were minimal.

TABLE 1. CHEMICAL ANALYSES OF ELEMENTS USED TO PREPARE MASTER ALLOYS

Impurity Element Reported	Major Impurity Content, Percent		
	Nickel, Baker Reagent Grade	Chromium, Electrolytic Grade	Aluminum, Alcoa
Fe	0.02	0.011	0.002
Si	--	0.014	0.002
C	--	0.005	--
Co	0.0002	--	--
Pb	0.004	--	--

The ingots were surface ground to remove imperfections that might have entrapped small amounts of slag. Alloy Number 1 was then crushed into small pieces by hand hammer. Alloys Number 2 and 3 showed somewhat more ductility and had to be crushed into smaller pieces with a hydraulic force hammer. These small pieces were then crushed using a diamond mortar to obtain a particle size of approximately 8.41×10^{-4} m (20 mesh). This coarse powder was then loaded in a steel ball mill and ground to obtain 7.4×10^{-5} m (-200 mesh) powder. Table 2 includes the melt data, weight loss, ball-mill time, and percent of powder recovery.

A pack-diffusion treatment was used to introduce the dopants Mn, Fe, or Co into the alloys or scales. The packs comprised 83% by weight alumina powder, 0.83% sodium chloride, 0.83% urea and 15.3% of the Mn-, Fe-, or Co-containing alloy powder. These powders were blended for 2.16×10^{4} s (6 h) then packed into small graphite boats with the coupons to be tested, and placed in the annealing furnace, which was flushed overnight with argon before the anneal was started. The coupons in the as-received condition were pickled in nitric acid before being introduced into the pack. Preoxidized specimens, used in an attempt to directly dope the scale, were simply degreased before introduction into the pack. After the annealing treatment, all coupons were washed in hot water, brushed, dried, and weighed.

In all, three separate pack diffusion runs were made, using the conditions in Table 3. After evaluation of coupons doped in Batch 1, iron was eliminated as a candidate dopant, and cobalt was eliminated after evaluation of the coupons from Batch 2. The Batch 3 conditions were used to dope both oxidation test coupons and tensile test coupons for the final analysis of the effects of the dopant on alloy properties.

The surfaces of the coupons after the pack annealing treatments were rough as a result of the presence of adherent nodules of alloy bearing a similar composition to the pack alloy. The incidence of protruberant nodules, as distinct from a fairly uniform layer, was greater on preoxidized coupons (Figures 2b, 2d, and 2f) than on coupons pack annealed in the as-received condition (Figures 2a, 2c, and 2e). The original surface of the coupon in Figure 2b is indicated by the arrows, and at high magnification before etching the preoxidized film was visible in this location. The white-etching layer beneath this surface in Figure 2b indicates either that manganese diffused through the surface scale, or that the surface scale was locally detached, allowing manganese access to the alloy. The arrows in Figure 2f indicate the paths of line-scans made with the electron microprobe.

These nodules comprised Ni, Cr, Al, and Mn, Co, or Fe, but no Th (Figure 3) and it was therefore concluded that they were pieces of the pack alloy. The voids shown in Figures 2d and 2f beneath the attached pack alloy were only observed in the cobalt- and iron-doped alloys.

The high manganese content of the white-etching surface layer in coupon BB is clearly shown in the electron-microprobe line traverse shown in Figure 4a.

The X-ray intensities obtained from these alloys were corrected for background, dead time, absorption, and fluorescence by comparison with X-ray data obtained from a chemically analyzed coupon of the as-received alloy.

TABLE 2. ARC MELT AND POWDER PREPARATION DATA FOR Ni-Cr-Al BASE ALLOYS (0.400 kg weight)

	Ingot Preparation				Powder Preparation				
					Time in Ball Mill		Weight of Powder Finer Than 7.4×10^{-5}m (-200 mesh),	Weight of Powder Coarser Than 7.4×10^{-5}m (+200 mesh),	
Alloy Composition	Times Melted	Melt Time, seconds	Final Weight, kg	Weight Loss, kg	Seconds	Hours	kg	kg	Powder Recovery, percent
Ni-15Cr-15Al-5Fe	2	540	0.39940	0.00060	1.872×10^5	52	0.325	0.020	81.4
Ni-15Cr-15Al-5Mn	2	600	0.39960	0.00040	2.448×10^5	68	0.385	Nil	96.4
Ni-15Cr-15Al-5Co	2	600	0.39910	0.00090	2.880×10^5	80	0.300	0.013	75.2

TABLE 3. PACK-ANNEALING CONDITIONS

Batch No.	Pack Doping Constituent	Temperature, °K	Time		Average Coupon Weight Gain, %
			Seconds	Hours	
1	Ni-15Cr-15Al-5Mn	1533	1.08×10^4	3	5.14 4.40*
1	Ni-15Cr-15Al-5Fe	1533	1.08×10^4	3	2.72 0.98*
1	Ni-15Cr-15Al-5Co	1533	1.08×10^4	3	2.21 0.47*
2	Ni-15Cr-15Al-5Mn	1573	3.6×10^3	1	4.41
2	Ni-15Cr-15Al-5Co	1573	3.6×10^3	1	2.13
3	Ni-15Cr-15Al-5Mn	1533	1.08×10^4	3	5.86 5.24**

* Preoxidized Coupons
** Tensile Test Coupons

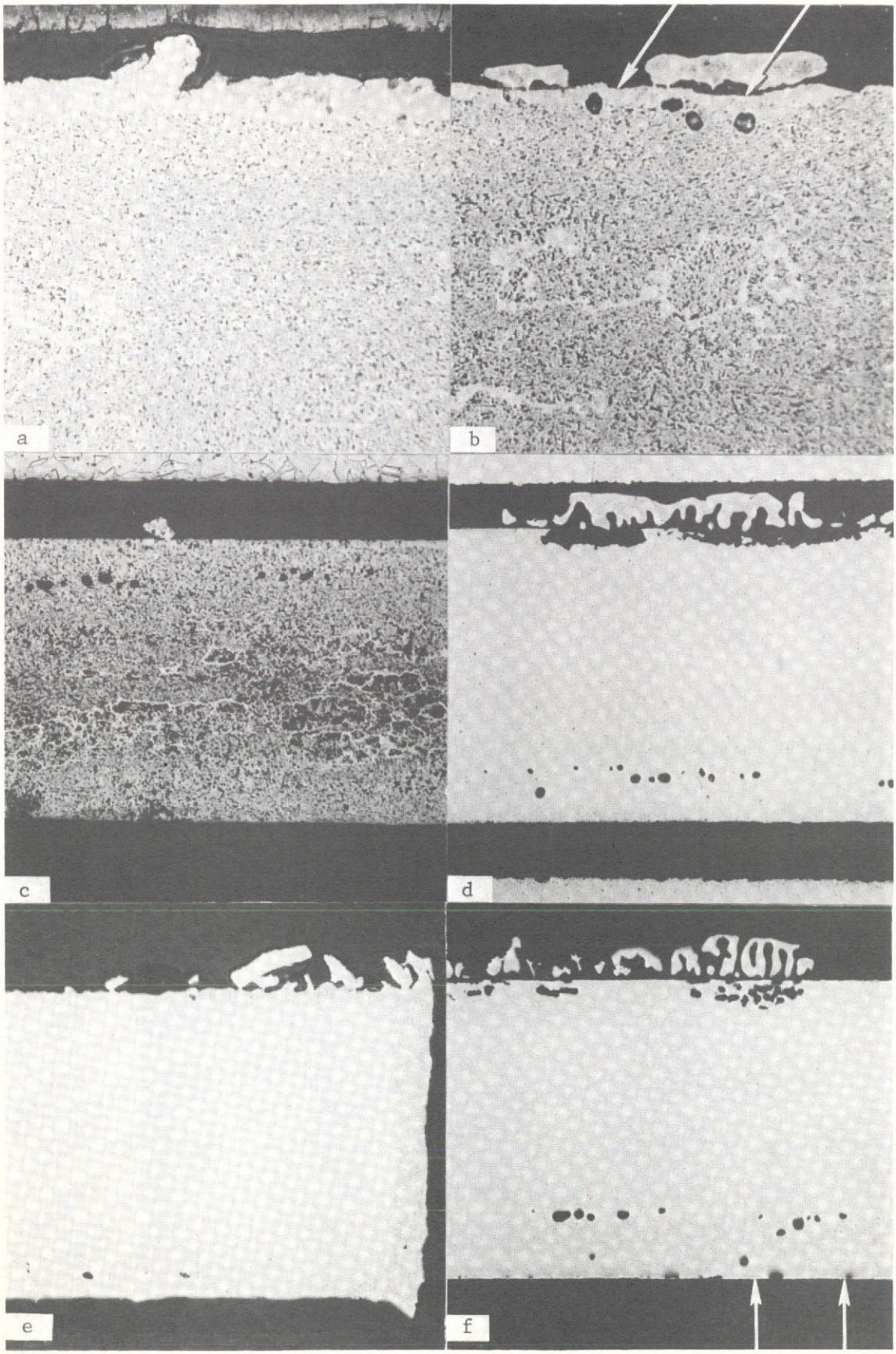

FIGURE 2. CROSS SECTIONS OF COUPONS AFTER PACK ANNEALING (a) DS NiCrAl-Mn No. BB, X500 (etched); (b) DS NiCrAl-Mn, No. B, X500 (etched); (c) DS NiCrAl-Co, No. FF, X200 (etched); (d) DS NiCrAl-Co, No. F, X200; (e) DS NiCrAl-Fe, No. KK, X200; (f) DS NiCrAl-Fe, No. K, X200.

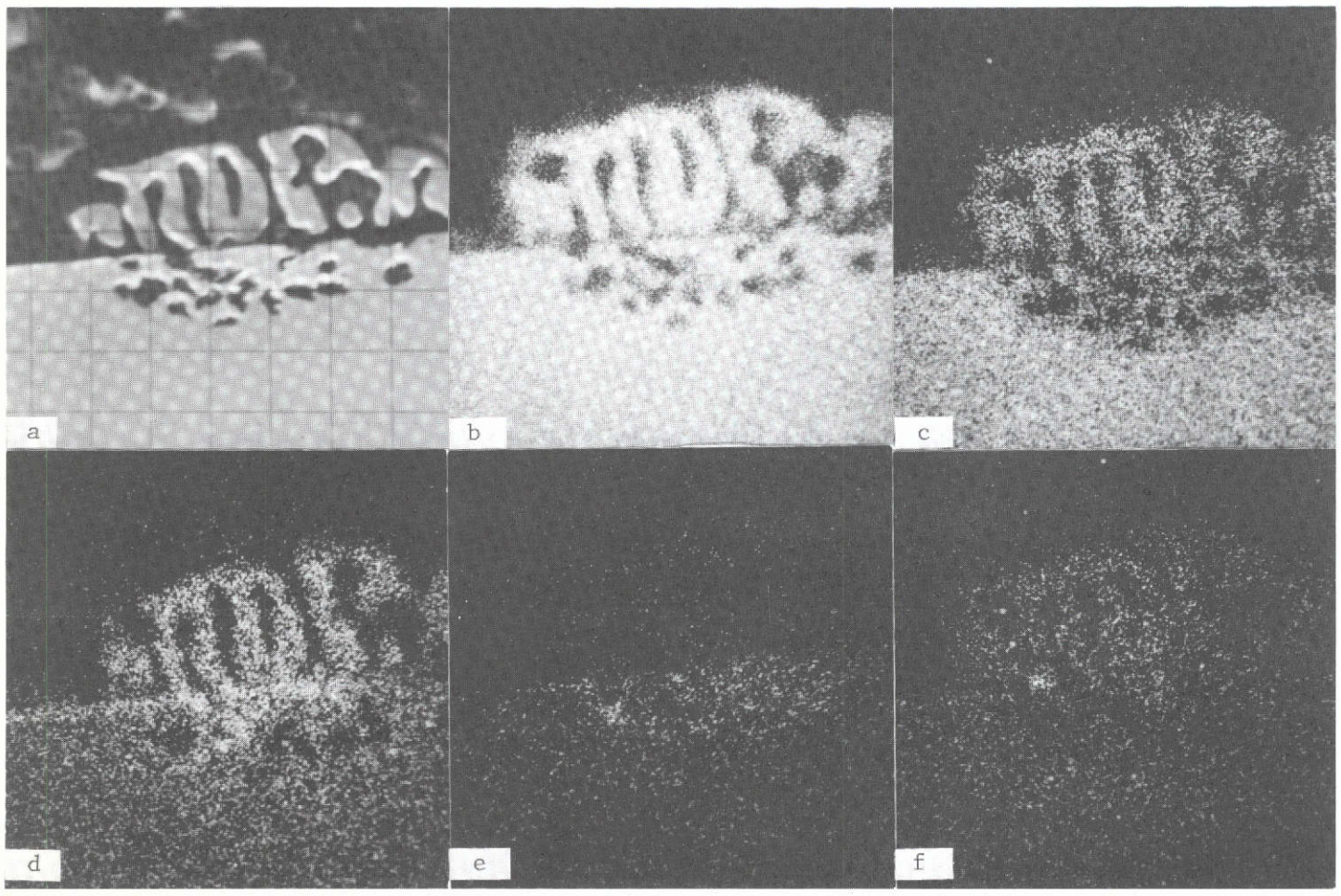

FIGURE 3. ELECTRON-PROBE MICROANALYSIS OF DS NiCrAl-Fe (No. K). Specimen preoxidized 1.8×10^4s (5h) at 1373°K (1100°C), 1.33×10^3 N/m^2 (10 torr) air, then pack annealed in Batch 1. All images X500. (a) Back scattered electron image; (b) Ni Kα X-ray image; (c) Cr Kα; (d) Al Kα; (e) Th Kα; (f) Fe Kα.

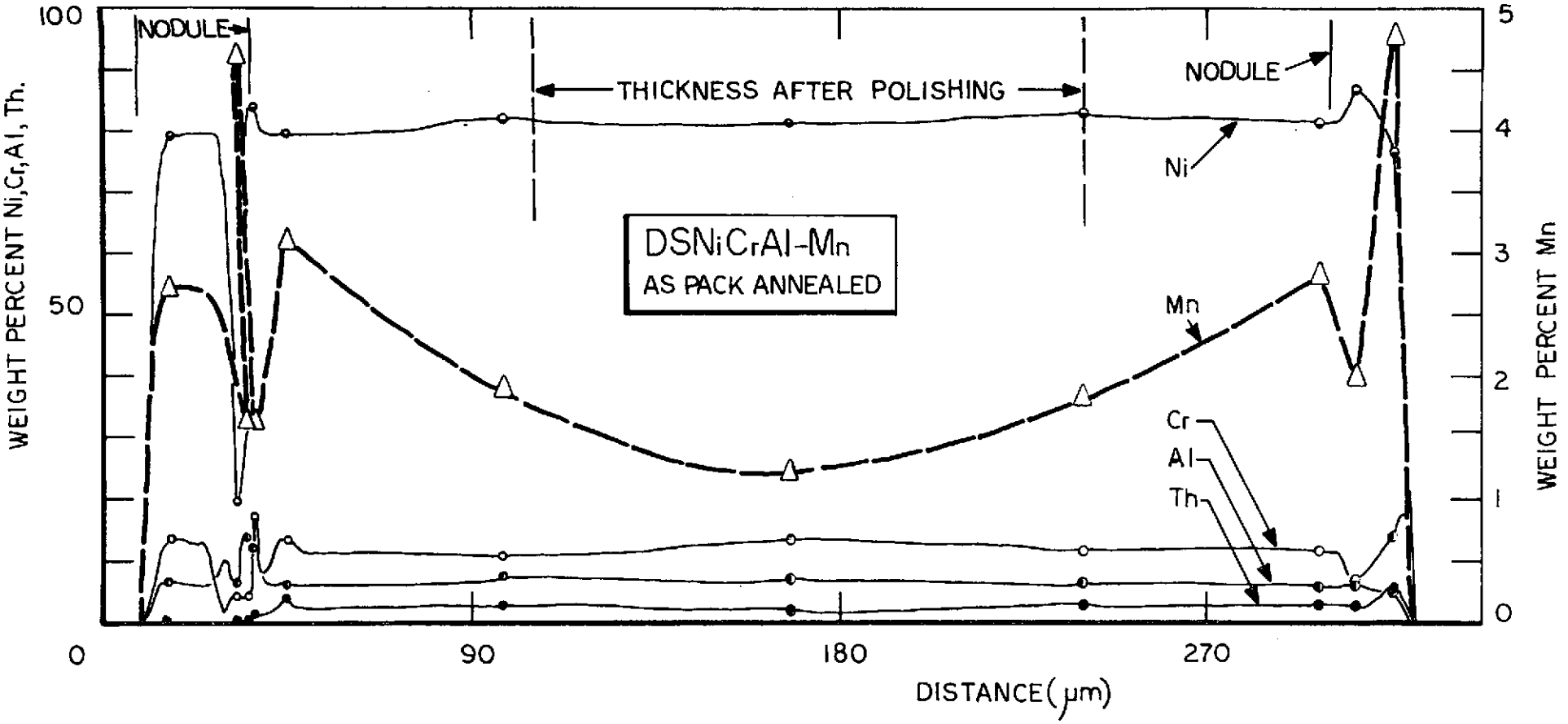

FIGURE 4a. CONCENTRATION PROFILE ACROSS THE THICKNESS OF DS NiCrAl-Mn (COUPON NO. BB) AFTER PACK ANNEALING IN BATCH 1

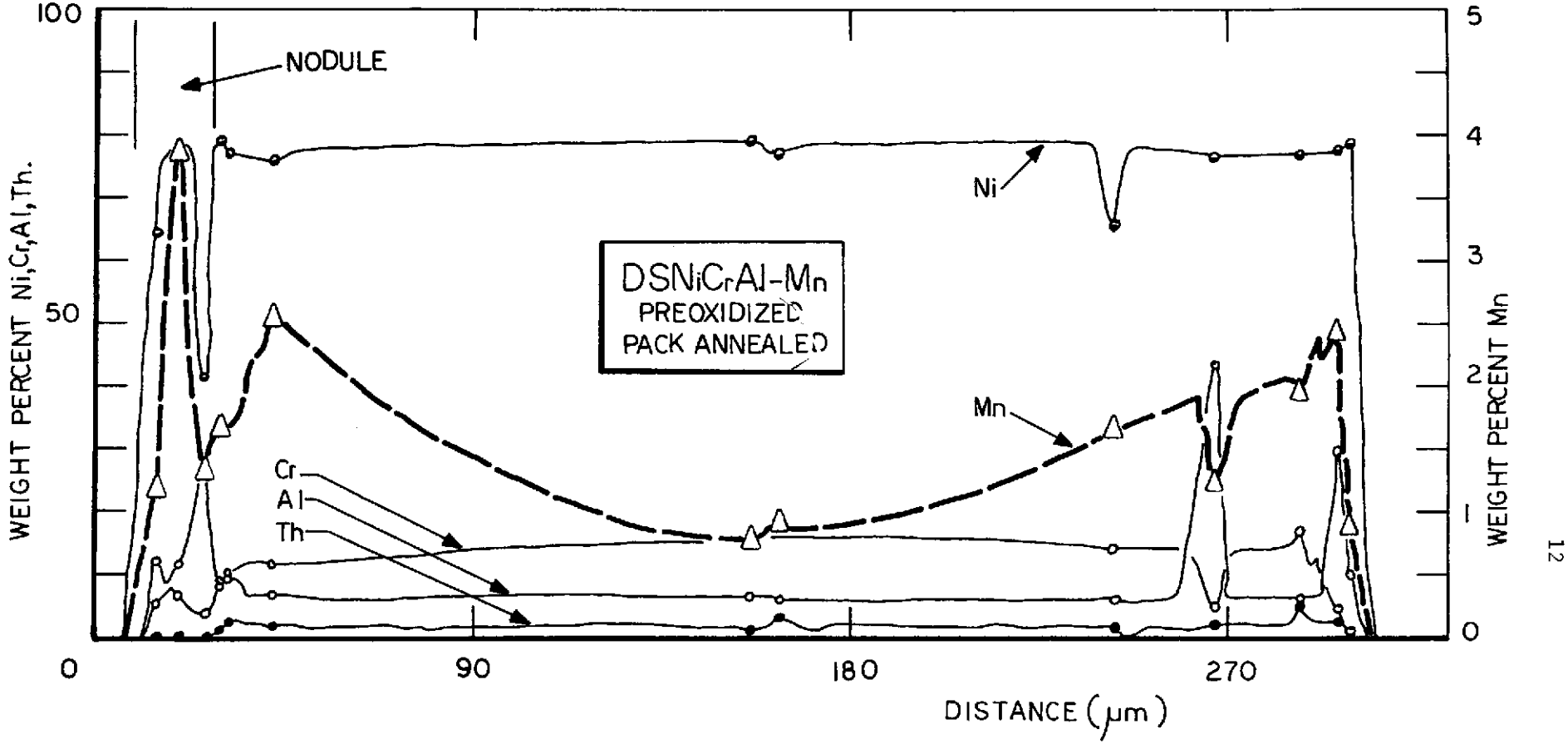

FIGURE 4b. CONCENTRATION PROFILE ACROSS DSNiCrAl-Mn (COUPON NO. B) AFTER PACK ANNEALING IN BATCH 1

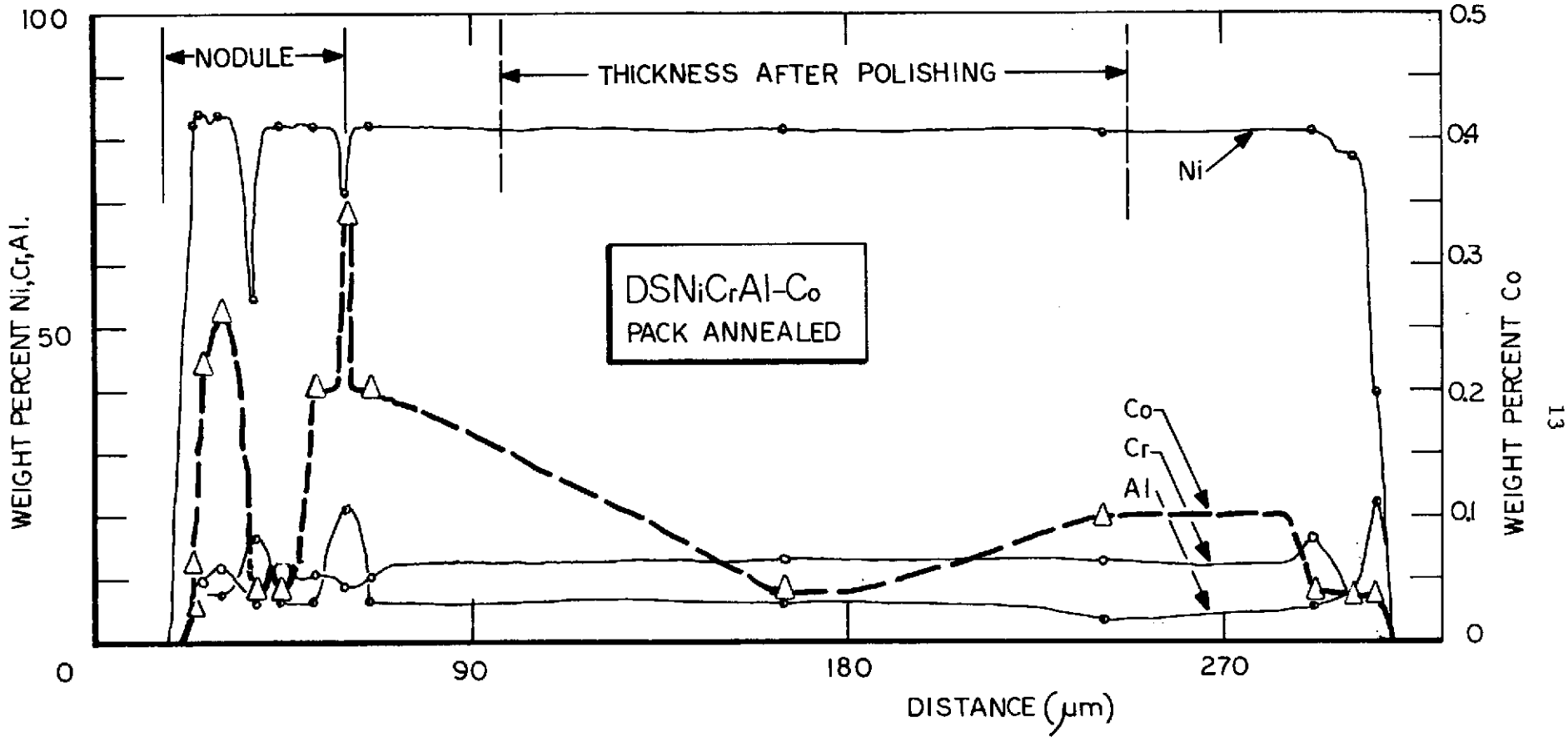

FIGURE 4c. CONCENTRATION PROFILE ACROSS THE THICKNESS OF DS NiCrAl-Co (COUPON NO. FF) AFTER PACK ANNEALING IN BATCH 1

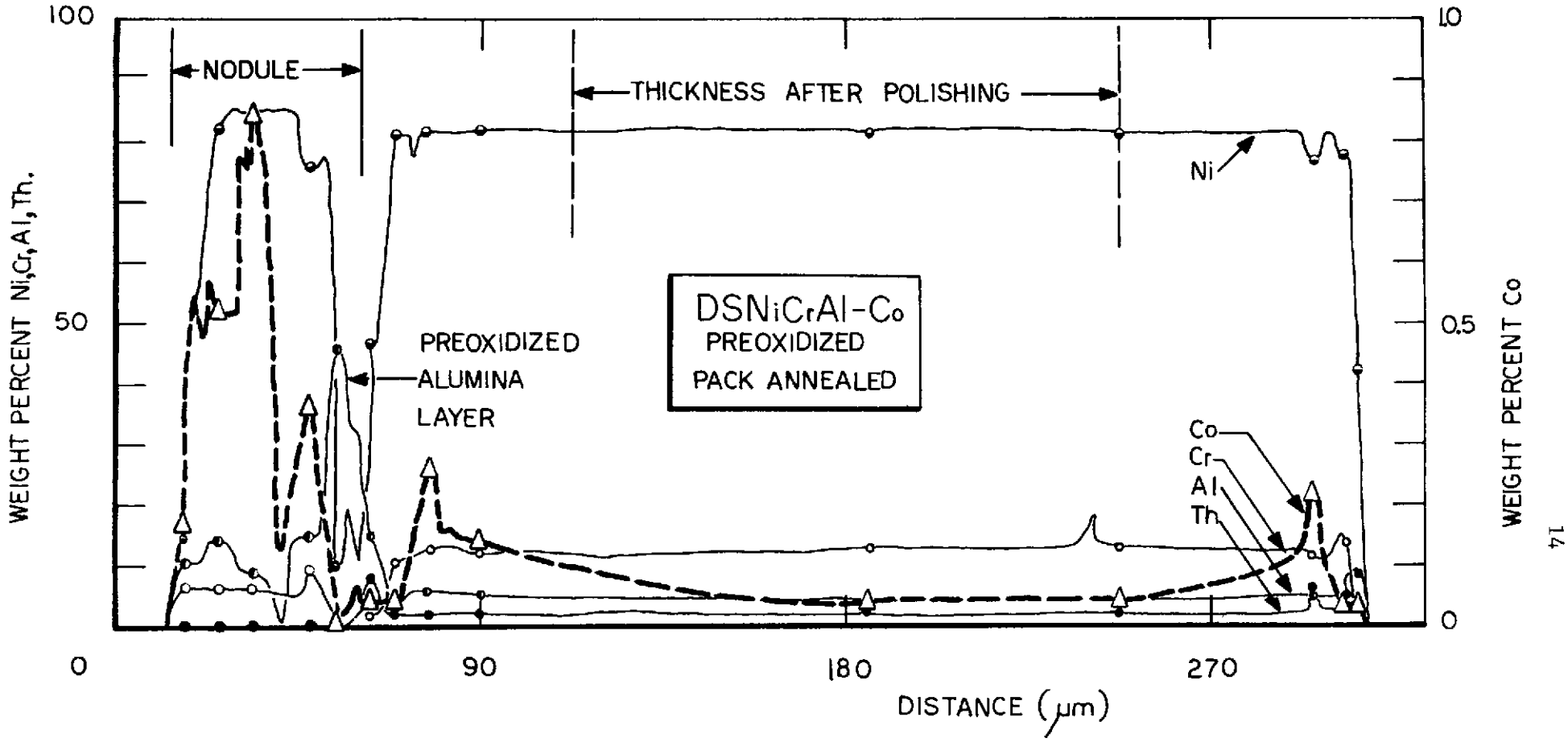

FIGURE 4d. CONCENTRATION PROFILE ACROSS THE THICKNESS OF DS NiCrAl-Co (COUPON NO. F) AFTER PACK ANNEALING IN BATCH 1

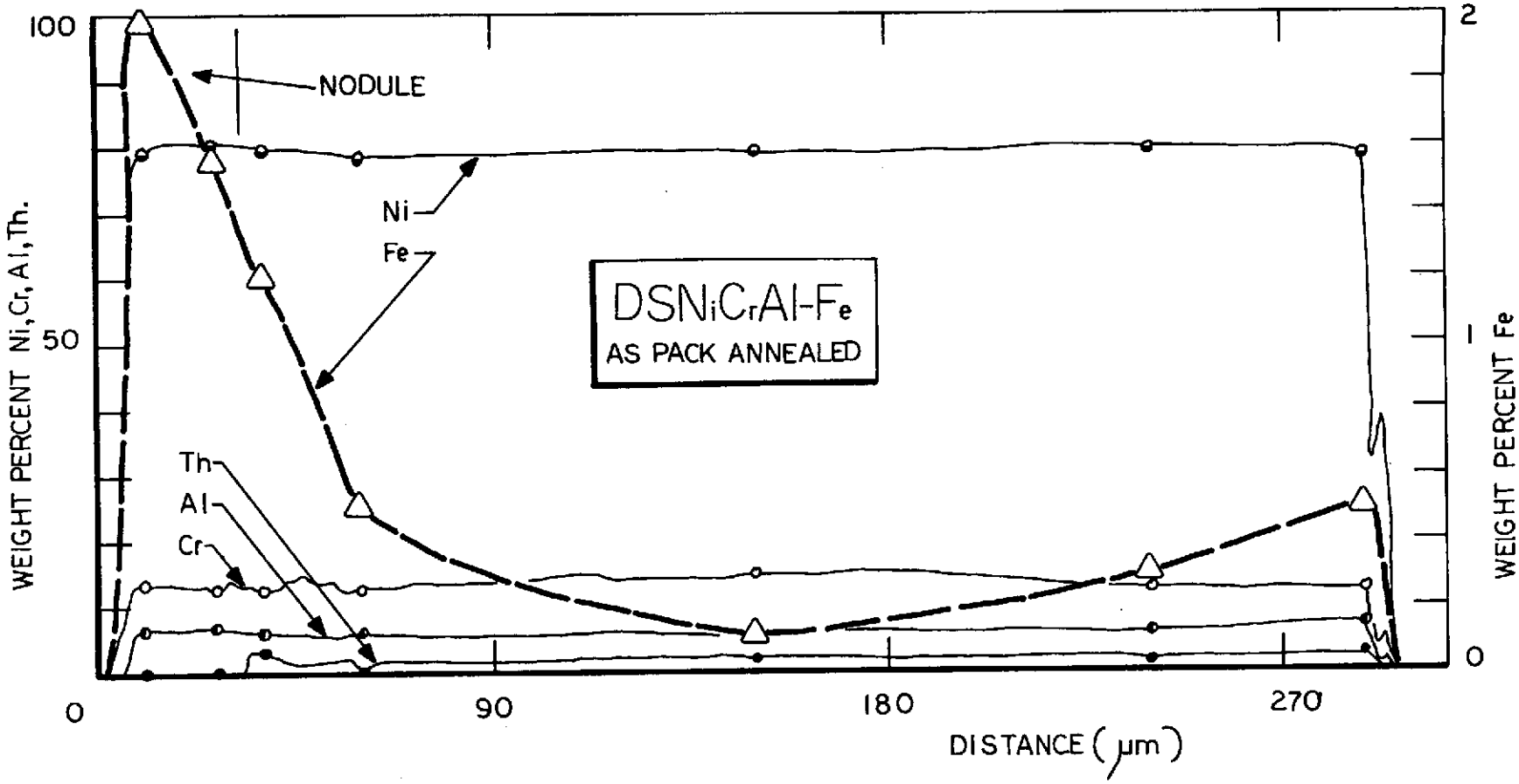

FIGURE 4e. CONCENTRATION PROFILE ACROSS DSNiCrAl-Fe (COUPON NO. KK) AFTER PACK ANNEALING IN BATCH 1

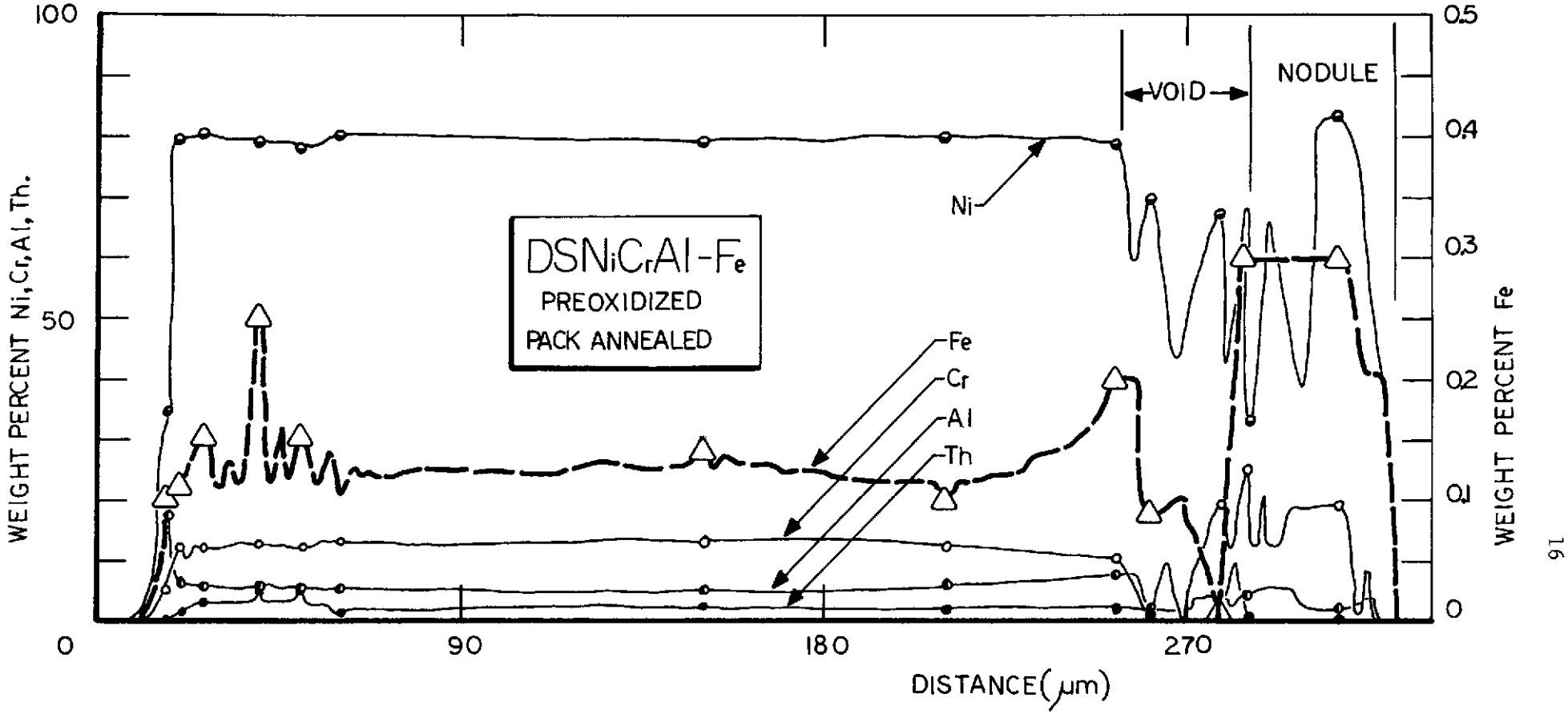

FIGURE 4f. CONCENTRATION PROFILE ACROSS DS NiCrAl-Fe (COUPON NO. K) AFTER PACK ANNEALING IN BATCH 1

Concentration profiles across the thickness of coupons from the Batch 1 treatments are shown in Figure 4, and from Batch 2 and 3 treatments in Figures 5 and 6, respectively.

In general, it proved to be relatively easy to introduce 1 to 4% of manganese into the alloy, whereas a maximum of only 0.34% cobalt and only 0.5% iron was measured at the surfaces of the other alloys after pack annealing. In addition, the aluminum levels of the pack annealed alloys were up to 1% higher than the as-received alloy after Batch 1 treatment, up to 4.6% higher after Batch 2 treatment, and up to 3.9% higher after Batch 3 treatment. These data are summarized in Table 4.

Because of the deposition of a layer of pack alloy even on top of preoxidized coupons, the concept of directly doping the oxide films by this method was discarded after Batch 1. A surprising feature was the apparent ease of penetration of the dopants, especially Mn, into the preoxidized coupons, which may reflect the mobility of Mn, Fe, and Co atoms in alumina, or may be an indication that the preformed oxides were unstable under the pack conditions. An interesting feature of the coupons from the Batch 2 pack annealing treatment was that the surfaces were relatively free of the nodular formations of adherent pack alloy found on the coupons after the Batch 1 and 3 annealing runs. The surface and edges of the manganese-doped alloy exhibited a microstructure different from that observed previously (Figure 7a), the white-etching areas polishing softer than the matrix. The microstructure of the cobalt-doped alloy (Figure 7b) was little changed from that of the undoped alloy.

Emittance Measurements

Total normal emittance measurements were made of pack annealed coupons which had been given an oxidation exposure after the doping treatment. These coupons were all metallographically ground and polished before oxidation to remove the adherent pack alloy nodules, and the thicknesses of these coupons after the grinding step is indicated in Figure 4.

The emittance measurements were made in vacuum at 1373 and 1473°K (some additional measurements were made at 773 and 1073°K), by comparison with a standard. The apparatus used is outlined in Figure 8. The two-part tantalum heater completely surrounds the specimen wheel. Three specimens, together with a standard, are mounted on the wheel, which rotates at about 0.7 rad/s. Radiation from a specimen as it passes the detector probe is transmitted through a hole in the probe to a thermopile detector. For this work, the detector was mounted in the position normal to the plane of the coupons, rather than in the first offset position as shown in Figure 8. The output of the thermopile is directly proportional to the thermal energy radiated from the specimen surface. The emittance was determined by direct comparison of irradiancy with that from the standard, which was a graphite disc with a contoured surface. Its emittance has been determined by comparison with an emittance standard issued by the National Bureau of Standards.

The results are listed in Table 5, and although the potential error in emittance values used for the standard may be as great as 10%, the emittance values are given to three figures to preserve the significance of the comparison.

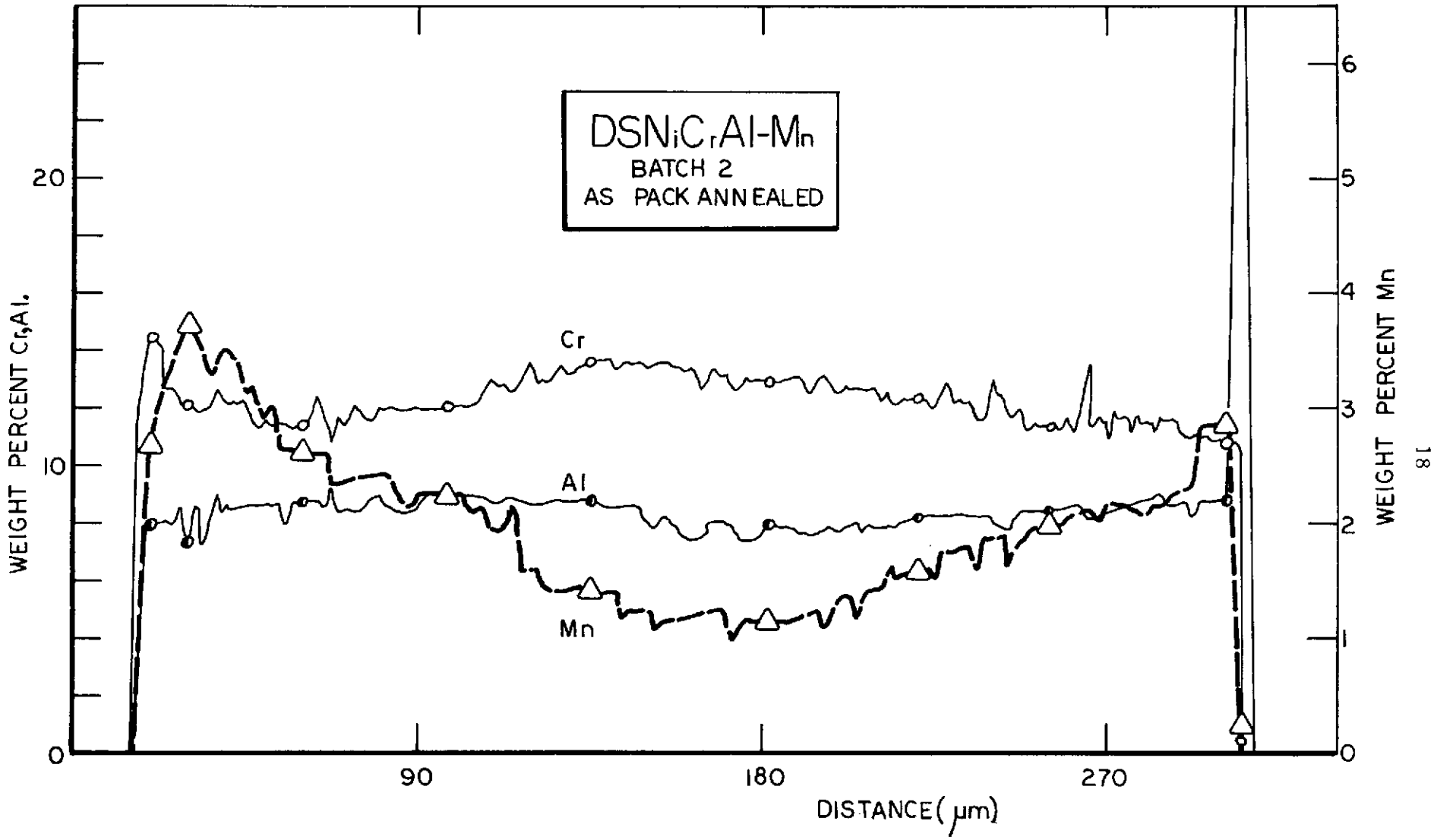

FIGURE 5a. CONCENTRATION PROFILE ACROSS THE THICKNESS OF DSNiCrAl-Mn COUPON FROM BATCH 2

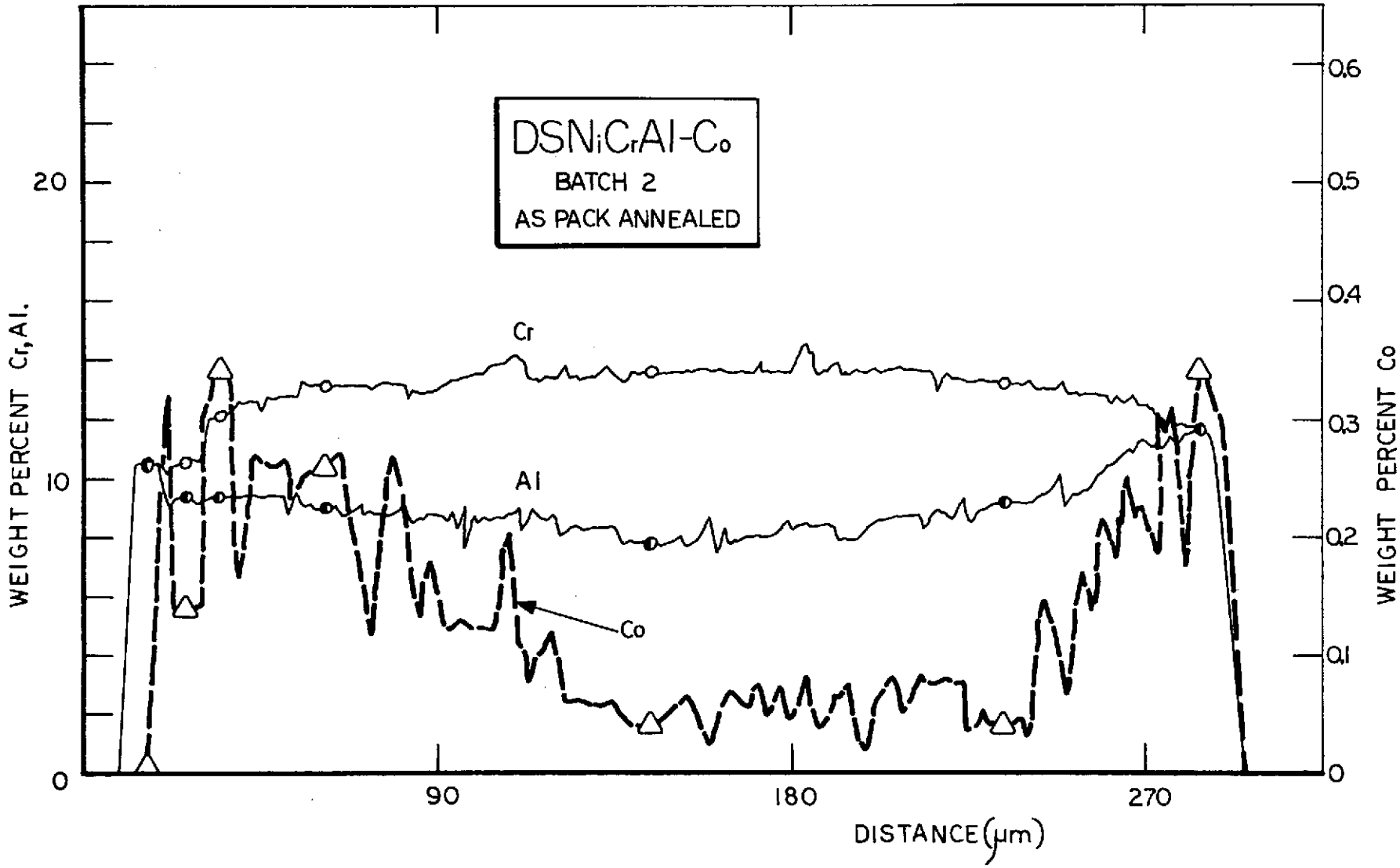

FIGURE 5b. CONCENTRATION PROFILE ACROSS THE THICKNESS OF DSNiCrAl-Co COUPON FROM BATCH 2

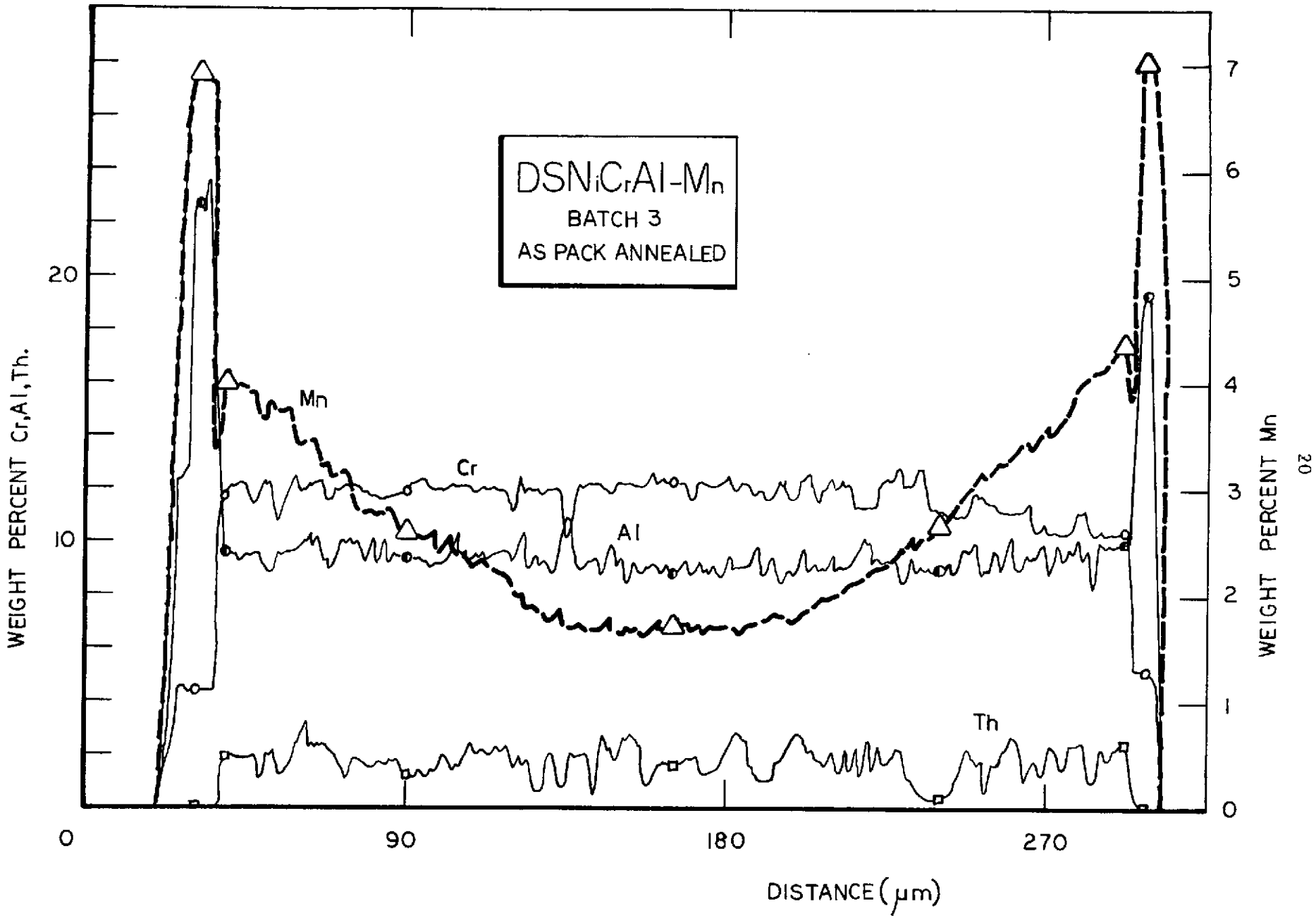

FIGURE 6. CONCENTRATION PROFILE ACROSS THICKNESS OF DSNiCrAl-Mn COUPON FROM BATCH 3

TABLE 4. SUMMARY OF CORRECTED ELECTRON MICROPROBE RESULTS

Alloy	Specimen Number	Treatment	Element	Concentration (w/o) Edge	Center
		Batch 1			
DS NiCrAl-Mn	BB	Pack annealed	Cr	12.5	13.2
			Al	6.3	7.0
			Mn	2.9	1.2
DS NiCrAl-Mn	B	Preoxidized, pack annealed	Cr	11.6	15.4
			Al	6.5	6.5
			Mn	2.5	0.8
DS NiCrAl-Co	FF	Pack annealed	Cr	11.6	12.9
			Al	6.7	6.5
			Co	0.15	0.04
DS NiCrAl-Co	F	Preoxidized, pack annealed	Cr	11.9	12.9
			Al	5.1	4.3
			Co	0.24	0.04
DS NiCrAl-Fe	KK	Pack annealed	Cr	12.7	14.8
			Al	6.8	6.0
			Fe	0.50	0.10
DS NiCrAl-Fe	K	Preoxidized, pack annealed	Cr	11.1	12.9
			Al	6.5	5.2
			Fe	0.23	0.14
		Batch 2			
DS NiCrAl-Mn		Pack annealed	Cr	11.4	13.6
			Al	8.4	8.0
			Mn	3.3	1.1
DS NiCrAl-Co		Pack annealed	Cr	11.9	13.6
			Al	10.5	7.8
			Co	0.34	0.04
		Batch 3			
DS NiCrAl-Mn		Pack annealed	Cr	11.0	12.3
			Al	9.8	8.8
			Mn	4.2	1.7

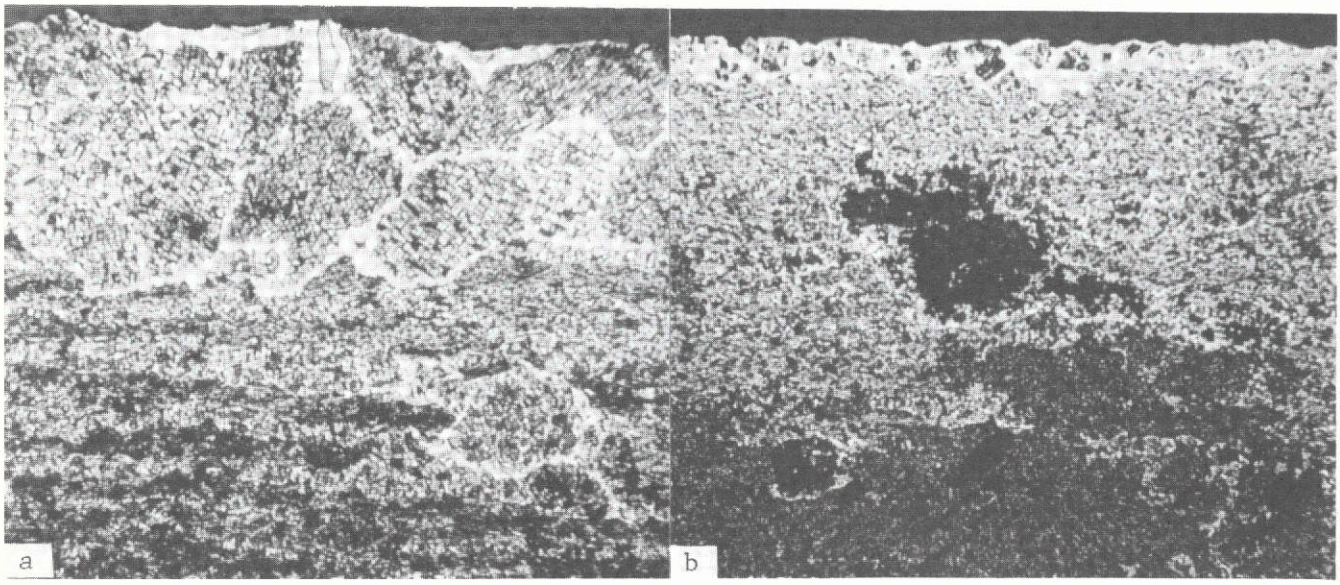

FIGURE 7. ETCHED CROSS SECTIONS OF DOPED (BATCH 2) DSNiCrAl ALLOYS

(a) DSNiCrAl-Mn, X500
(b) DSNiCrAl-Co, X500.

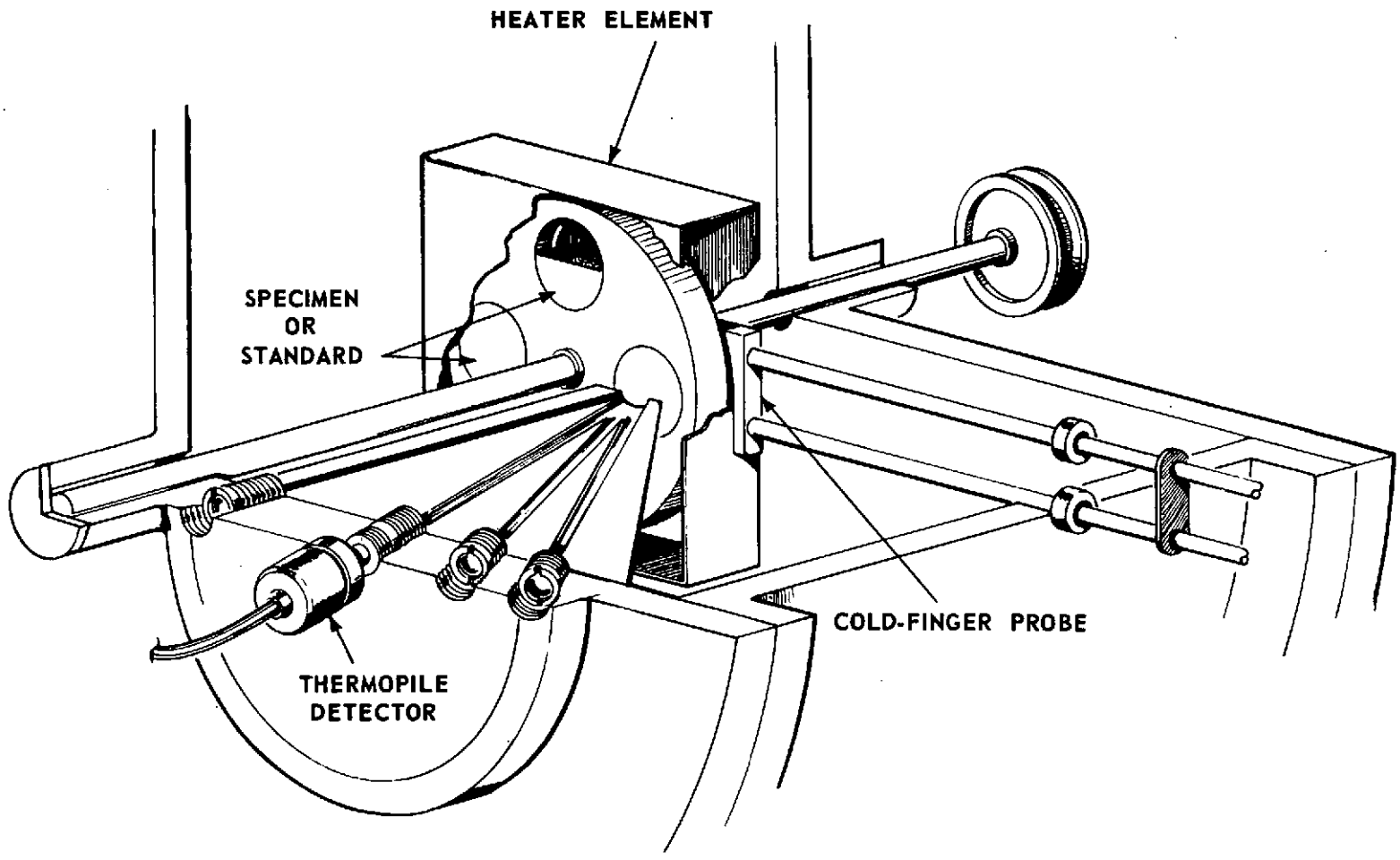

FIGURE 8 . COMPARATIVE TOTAL EMITTANCE APPARATUS

TABLE 5. TOTAL NORMAL EMITTANCE MEASUREMENTS

Alloy	Specimen Number	Treatment	Temperature, °K 1373	1473
DSNiCrAl	7	Oxidized 2.02×10^5s (56h), 1473°K, 1.33×10^3 N/m^2 (10 torr) air	0.485	0.504
	20	Oxidized 1.84×10^5s (51h), 1373°K, 1.33×10^3 N/m^2 (10 torr) air	0.427	0.446
DSNiCrAl	27	Polished to Linde B, oxidized 2.34×10^5s (65h), 1373°K, 1.33×10^4 (100 torr) oxygen	0.631	0.669
		Batch 1		
DSNiCrAl-Mn	17-C	Preoxidized, pack annealed, polished to Linde B, oxidized 1.55×10^5s (43h) 1473°K, 1.33×10^3 N/m^2 (10 torr) air	0.582	0.592
DSNiCrAl-Mn	31-D	Preoxidized, pack annealed, polished to 240 grit, oxidized 1.87×10^5s (52h) 1473°K, 1.33×10^3 N/m^2 (10 torr) air	0.574	0.590
DSNiCrAl-Co	16-EE	As pack annealed, oxidized 1.8×10^5s (50h) 1473°K, 1.33×10^3 N/m^2 (10 torr) air	0.568	0.540
DSNiCrAl-Co	34-GG	Pack annealed, polished to Linde B, oxidized 1.84×10^5s (51h), 1473°K, 1.33×10^3 N/m^2 (10 torr) air	0.612	0.654
DSNiCrAl-Co	36-HH	Pack annealed, polished to Linde B, oxidized 1.76×10^5s (98 cycles) 1473°K, 1.33×10^3 N/m^2 (10 torr) air	0.476	0.470
DSNiCrAl-Co	33-G	Preoxidized, pack annealed, polished to Linde B, oxidized 2.02×10^5s (112 cycles) 1473°K, 1.33×10^3 N/m^2 (10 torr) air	0.530	0.536
DSNiCrAl-Fe	42-LL	Pack annealed, polished to Linde B, oxidized 2.52×10^5s (70h) 1473°K, 1.33×10^3 N/m^2 (10 torr) air	0.606	0.611
DSNiCrAl-Fe	39-J	Preoxidized, pack annealed, polished to 240 grit, oxidized 2.59×10^5s (72h) 1473°K, 1.33×10^3 N/m^2 (10 torr) air	0.442	0.460

TABLE 5. Continued

Alloy	Specimen Number	Treatment	Temperature, °K 1373	1473
		Batch 2		
DSNiCrAl-Mn	60	Pack annealed, polished to 600 grit, oxidized 2.54×10^5s (141 cycles) 1473°K, 1.01×10^3 N/m^2 (760 torr) air	0.497	0.504
DSNiCrAl-Co	58	Pack annealed, polished to 600 grit, oxidized 2.23×10^5s (62h) 1473°K, 1.01×10^5 N/m^2 (760 torr) air	0.509	0.522
DSNiCrAl-Co	59	Pack annealed, polished to 600 grit, oxidized 1.78×10^5s (99 cycles) 1473°K, 1.01×10^5 N/m^2 (760 torr) air	0.503	0.518
		Batch 3		
DSNiCrAl-Mn	68	Pack annealed, polished to 600 grit, oxidized 1.78×10^5s (99.5 cycles) 1373°K, 1.33×10^3 N/m^2 (10 torr) air	0.518	--
DSNiCrAl-Mn	96	Pack annealed, polished to 600 grit, oxidized 1.82×10^5s (101 cycles) 1473°K 1.33×10^3 N/m^2 (10 torr) air	0.567	--
TDNiCr[5]	(66)	Oxidized 2.29×10^5s (127 cycles) 1473°K, 1.01×10^5 N/m^2 (760 torr) air	0.678	0.687
TDNiCr[5]	(36)	Oxidized 1.67×10^5s (93 cycles) 1473°K, 1.33×10^3 N/m^2 (10 torr) air	0.673	--

An overall analysis of the emissivity changes affected by the three dopants used suggests that manganese additions to the alloy result in a modest (17-19%) increase which is, however, thermally stable, whereas somewhat greater increases can be obtained with cobalt and iron additions if the oxidation conditions are such that the transient oxides containing these elements can form and remain in the scale. Under conditions unfavorable to the production of transient oxides (rough surface finish, low oxygen pressure) or unfavorable to their retention in the scale (thermal cycling), the emittance of the scales on the cobalt- and iron-doped alloys is the same as that of the undoped alloy. When the undoped alloy is oxidized to produce considerable amounts of transient oxides, the final scale is green-blue instead of grey, and the emittance is in fact greatly increased (coupon No. 27 in Table 5). This effect is practically achieved by the use of a highly-polished (Linde B) surface finish on the coupon before oxidation. Commercially it may be cheaper to incorporate a small amount of manganese during alloy preparation than to polish the finished sheet.

The values of the emittance of manganese-doped DSNiCrAl are some 14% lower than the total normal emittance determined for TDNiCr which was oxidized to form a chromia scale. Recent, independently-determined values of the total hemispherical emittance of TDNiCr[7], oxidized to form a chromia scale, are near to 0.73 (±0.07), while under conditions where NiO is the likely scale, the emittance is increased to around 0.83.

This is an interesting comparison, because the target value of emittance for this program is 0.85, which was the value of spectral emittance measured by Centolanzi[2] for the scale formed on TDNiCr at 1473°K (1200°C) in a hypervelocity air stream. Under these same conditions the emissivity of an alumina-forming TDNiCrAlY alloy was 0.70 ± 0.05. Consideration of available emissivity data suggests that either this high value measured for TDNiCr resulted from the formation of a NiO rather than a Cr_2O_3 scale on the alloy, or that the values reported by Centolanzi were considerably in error on an absolute scale, which is possible for emittance measurements made under adverse conditions.

For alloys which form thin, protective scales it is likely that the whole of the emissive source is not enclosed in the scale, but overlaps into the base metal. When this is the case, the concept of a highly-emissive, thin protective scale is practically limited by the contribution of the metal part of the composite to the measured, overall emissivity. Accordingly, a more realistic goal for this program might be to increase the emittance of oxidized DSNiCrAl sheet to that of TDNiCr sheet oxidized to produce a chromia scale, that is, to around 0.7.

III. EVALUATION TESTS

Oxidation Studies

Experimental Procedure

The alloys were oxidized at 1373 and 1473°K (1100 and 1200°C) in slowly-flowing dry air at 1.33×10^3 and 1.01×10^5 N/m^2 (10 and 760 torr) for times up to 3.24×10^5 s (90 h) in both isothermal and cyclic modes. The

oxidation apparatus has been described previously[5]. The isothermal oxidation unit comprised a Cahn RG or RH recording microbalance from which the coupons were suspended into a reaction tube in which the pressure of slowly-flowing air was maintained at a desired pressure. Oxidation tests in these thermobalances were initiated by raising a heated furnace around the reaction tube (RG balance), or dropping the coupon into a heated furnace by a magnetic device (RH balance). The cyclic oxidation unit was essentially the same as the RG-equipped balance described, thermal cycling being achieved by automatically raising and lowering a heated furnace around the reaction tube according to a pre-set program.

In most of the work the undoped alloy was oxidized with the as-received (belt sanded) surface finish, but a few runs were made with a polished (Linde B - 3×10^{-8} m) surface. The coupons of the doped alloys were oxidized with various surface finishes which will be described in a later section. Some additional work was done with the undoped alloy in 1.33×10^4 N/m^2 (100 torr) oxygen.

Results and Discussion

1. Kinetics of Undoped DSNiCrAl. The complete oxidation test data for this alloy are listed in Table 6, and the kinetic curves are shown in Figures 9a to 9d. As is immediately apparent, the oxidation kinetics were quite reproducible for a given set of conditions.

By comparison of the isothermal and cyclic curves at a specific temperature and pressure, it is clear that in general the adhesion of the scale to this alloy is excellent. Some slight spallation of scale occurred from all the specimens oxidized with an as-received (surface ground) finish, the scale being lost from the peaks of grinding grooves. When a smoother surface finish was employed, scale spallation was virtually eliminated (Table 6).

The oxidation rate of this alloy did not always follow a parabolic rate law. The initial oxidation was often near parabolic but the rate generally slowed to nearer cubic (or higher index) after 1.08×10^4 to 3.6×10^4 s (3 to 10 h). Parabolic rate constants calculated from the observed instances of parabolic oxidation are summarized in Table 7.

For comparison, the parabolic rate constants for the oxidation of a dispersion-free, alumina-forming Ni-25%Al alloy at 1373 and 1473°K (1100 and 1200°C) in 1.01×10^4 N/m^2 (76 torr) oxygen were reported by Pettit[8] to be 6.5×10^{-11} kg^{2}m^{-4}s^{-1} and 7.0×10^{-10}kg^{2}m^{-4}s^{-1} respectively, while for alumina-forming, dispersion-free Ni-Cr-Al alloys, Giggins and Pettit[9] measured parabolic rate constants of 8.0×10^{-11} to 4.0×10^{-10}kg^{2}m^{-4}s^{-1}, and 7.0×10^{-10} to 1.5×10^{-9}kg^{2}m^{-4}s^{-1} at 1373 and 1473°K (1100 and 1200°C), respectively. Stott and Wood[10] have reported "crude" parabolic rate constants of 1.2×10^{-10} and 2.5×10^{-10}kg^{2}m^{-4}s^{-1} for the later stages of oxidation of a dispersion-free Ni-15%Cr-4%Al alloy at 1273 and 1473°K (1000 and 1200°C) respectively, in 1.01×10^5 N/m^2 (760 torr) oxygen. Although the rate constants observed for DSNiCrAl are up to an order of magnitude faster than for the Ni-25%Al alloy, they are almost the same as those for the alumina-forming Ni-Cr-Al alloys, indicating that the thoria dispersion exerts little effect on the oxidation rate of this alloy.

TABLE 6. OXIDATION TEST DATA FOR DSNiCrAl ALLOY

Specimen No.	Temperature		Air Pressure		Exposure Time		Weight Change ($kg/m^2 \times 10^2$)		Rate* Index (n)	Parabolic Rate Constant (kp) in kg^2/m^4 s
	^oK	^oC	N/m^2	torr	s	h	Cahn	Before & After		
8	1373	1100	1.33×10^3	10	3.6×10^3	1	0.084	0.075	--	--
28	1373	1100	1.33×10^3	10	1.66×10^5	46	0.479	0.489	2.5 (0-10h) 2.8 (10-46h)	--
9	1373	1100	1.33×10^3	10	1.73×10^5	48	D	0.244	--	--
20	1373	1100	1.33×10^3	10	1.84×10^5	51	0.511	0.499	2.2	1.4×10^{-10}
10	1373	1100	1.33×10^3	10	1.94×10^5	54	0.241	0.304	4.9	--
23	1373	1100	1.33×10^3	10	2.3×10^5	64	D	0.554	--	--
48	1373	1100	1.33×10^3	10	2.52×10^5	70	0.441	0.427	2.0 (0-8h) 2.6 (8-70h)	1.3×10^{-10}
27	1373	1100	1.33×10^4	100[A,B]	2.34×10^5	65	0.622	0.645	3.5	--
3	1373	1100	1.01×10^5	760	1.76×10^5	49	0.339	0.420	3.6	--
29	1373	1100	1.01×10^5	760[A]	1.87×10^5	52	0.576	0.566	2.4 (0-3h) 3.9 (3-50h)	6.4×10^{-10}
4	1373	1100	1.01×10^5	760	2.3×10^5	64	0.278	0.413	4.5	--
26	1373	1100	1.33×10^3	10	1.44×10^5	40C	0.380	0.400	--	--
25	1373	1100	1.33×10^3	10	1.8×10^5	50C	0.197	0.400	--	--
66	1373	1100	1.33×10^3	10	2.05×10^5	57C	0.527	0.446	--	--
24	1373	1100	1.01×10^5	760	2.02×10^5	56C	0.610	0.601	--	--
19	1373	1100	1.01×10^5	760	2.48×10^5	69C	0.571	0.566	--	--
62	1473	1200	1.33×10^3	10	9.0×10^4	25	0.880	0.625	1.5 (0-2.5h) 2.5 (7-25h)	--
11	1473	1200	1.33×10^3	10	1.8×10^5	50	0.904	0.774	2.0 (0-6h) 2.6 (6-50h)	7.2×10^{-10}
54	1473	1200	1.33×10^3	10	1.8×10^5	50	0.994	0.855	1.0 (0-1h) 3.3 (1-50h)	--
87A	1473	1200	1.33×10^3	10	1.84×10^5	51	1.074	0.729	2.0 (0-10h) 2.6 (10-51h)	1.1×10^{-9}
7	1473	1200	1.33×10^3	10	2.34×10^5	65	0.973	0.878	2.2	5.7×10^{-10} (0-12h) 4.1×10^{-10} (12-65h)

TABLE 6. Continued

Specimen No.	Temperature		Air Pressure		Exposure Time		Weight Change ($kg/m^2 \times 10^2$)		Rate* Index (n)	Parabolic Rate Constant (kp) in kg^2/m^4 s
	°K	°C	N/m^2	torr	s	h	Cahn	Before & After		
51	1473	1200	1.33×10^3	10	2.38×10^5	66	0.715D	0.505	--	--
30	1473	1200	1.33×10^4	100[A,B]	1.8×10^5	50	1.090	1.090	2.2 (0-3h) 3.0 (3-50h)	1.7×10^{-9}
46	1473	1200	1.01×10^5	760	6.0×10^2	0.2	0.030	0.064	--	--
63	1473	1200	1.01×10^5	760	6.0×10^2	0.2	--	0.118	--	--
43	1473	1200	1.01×10^5	760	1.08×10^4	3	0.153	0.350	2.0	1.5×10^{-10}
44	1473	1200	1.01×10^5	760	1.76×10^5	49	0.501D	0.504	--	--
5	1473	1200	1.01×10^5	760	1.84×10^5	51	0.889	0.907	2.8	--
50	1473	1200	1.01×10^5	760	1.84×10^5	51	0.329D	0.294	--	--
1	1473	1200	1.01×10^5	760	2.27×10^5	63	--	0.985	--	--
45	1473	1200	1.01×10^5	760	2.56×10^5	71	0.642D	0.518	--	--
49	1473	1200	1.01×10^5	760	3.24×10^5	90	0.959	0.835	2.4 (0-4h) 2.7 (4-90h)	7.9×10^{-10}
21	1473	1200	1.33×10^3	10	2.0×10^5	55.5C	0.923	0.874	--	--
22	1473	1200	1.33×10^3	10	2.03×10^5	56.5C	1.153	1.150	--	--
47	1473	1200	1.33×10^4	100[A,B]	2.03×10^5	56.5C	1.185	1.250	--	--
2	1473	1200	1.01×10^5	760	1.78×10^5	49.5C	--	0.830	--	--
6	1473	1200	1.01×10^5	760	1.8×10^5	50C	0.786	0.867	--	--
12	1473	1200	1.01×10^5	760	2.0×10^5	55.5C	0.754	0.795	--	--

* From $w^n = k.t$ where w = weight gain, t = time, n and k are constants. For parabolic oxidation, n = 2 and k = kp.

A. Linde B (0.03 μm) surface finish
B. Oxidized in oxygen
C. Cyclic oxidation, 1 cycle ≡ 1.8×10^3s at temperature
D. Balance malfunction

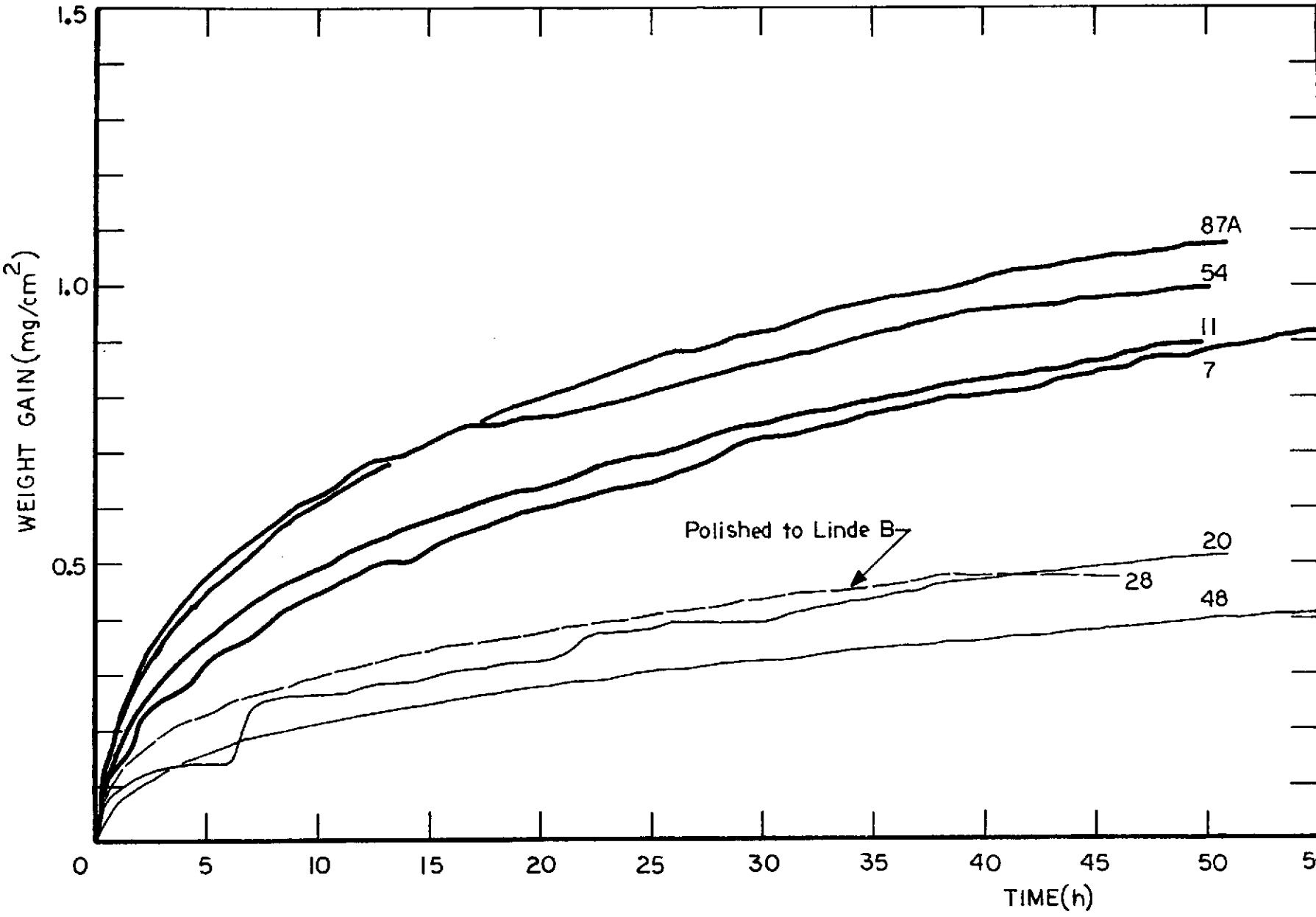

FIGURE 9a. ISOTHERMAL OXIDATION KINETICS OF DSNiCrAl IN 1.33×10^3 N/m^2 (10 TORR) AIR. THE BOLD LINES INDICATE THE RESULTS AT 1473°K (1200°C). THE LIGHT LINES AT 1373°K (1100°C).

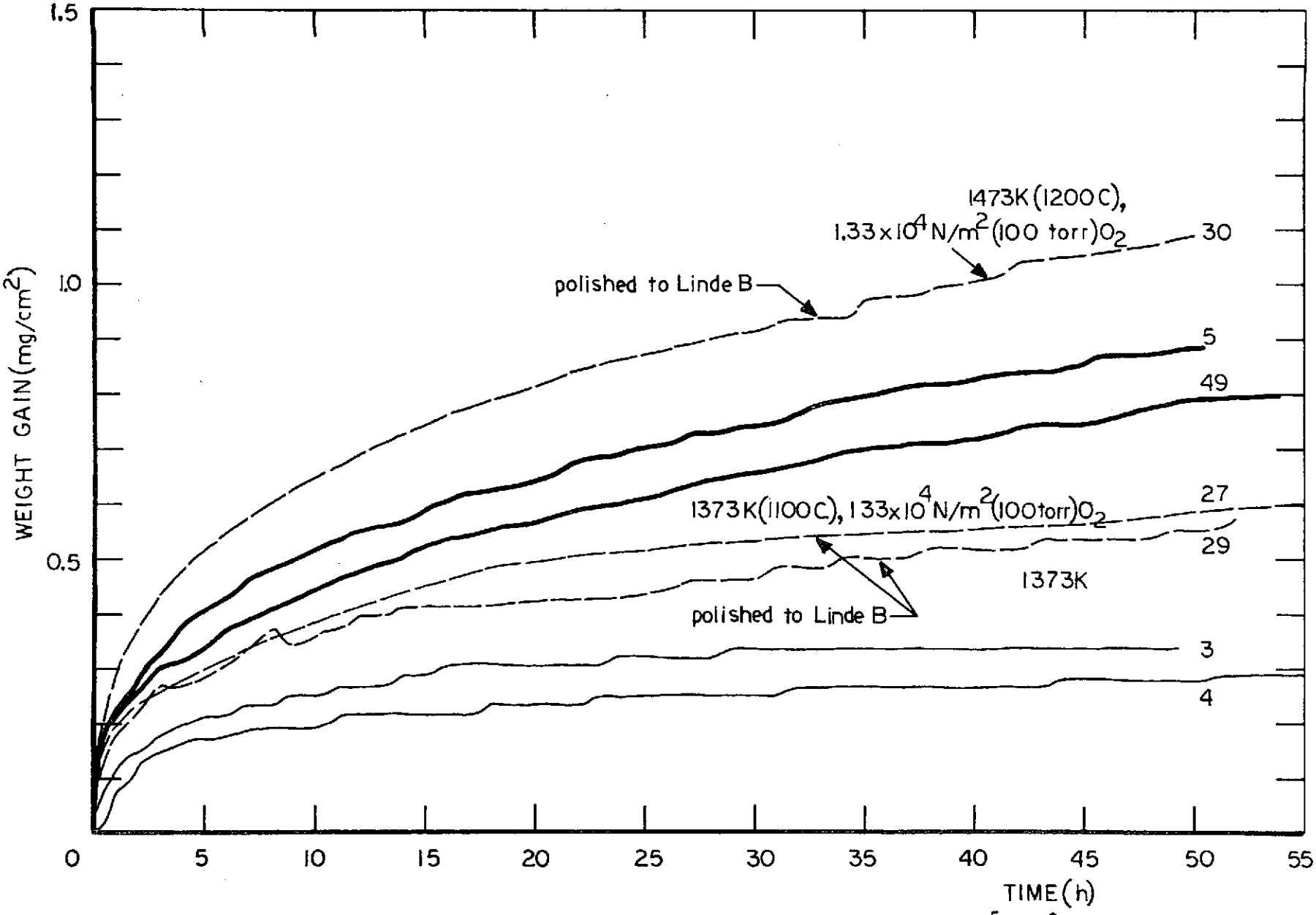

FIGURE 9b. ISOTHERMAL OXIDATION KINETICS OF DSNiCrAl IN 1.01×10^5 N/m^2 (760 TORR) AIR. THE BOLD, FULL LINES INDICATE THE KINETICS AT 1473°K (1200°C). THE LIGHT, FULL LINES AT 1373°K (1100°C).

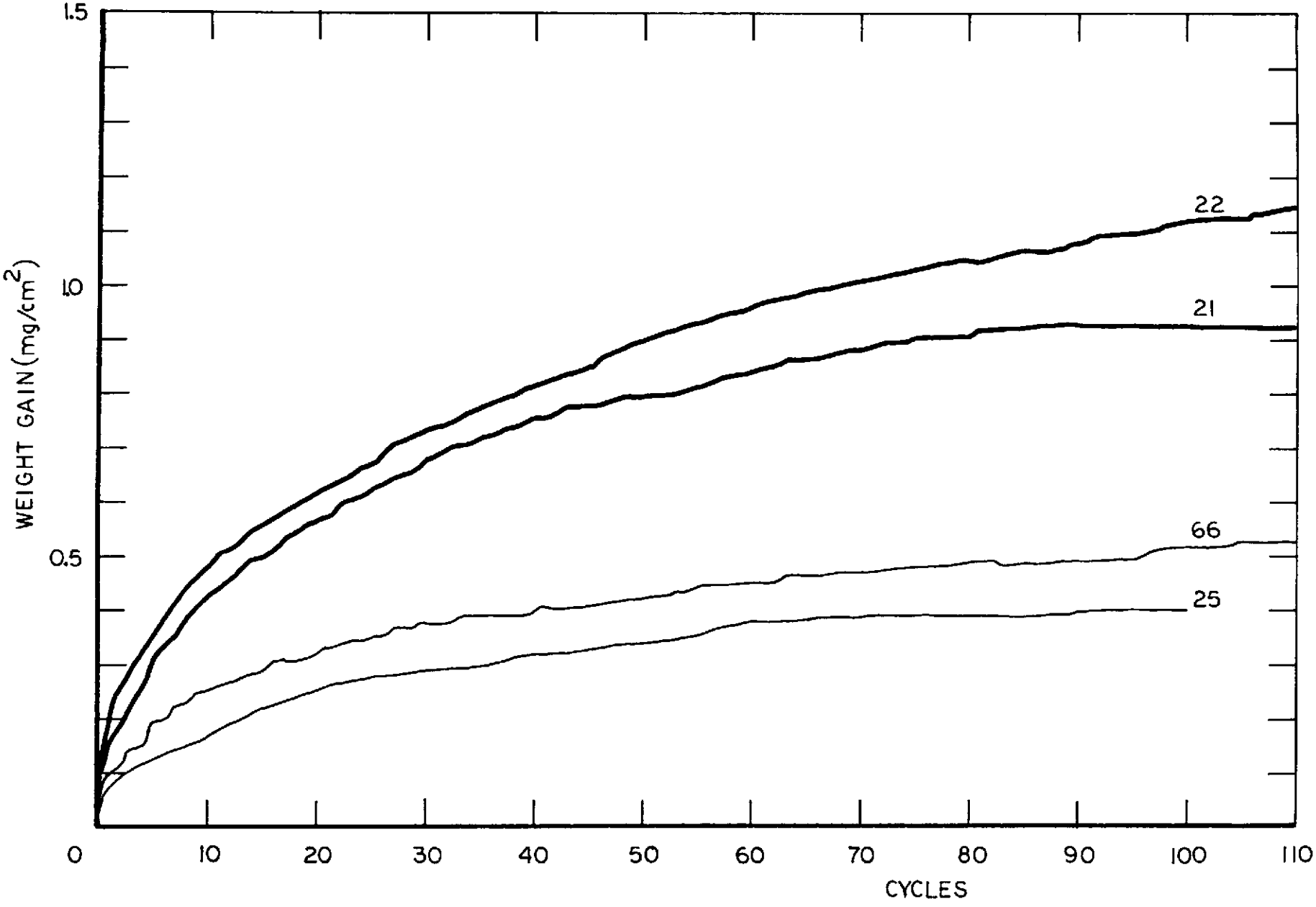

FIGURE 9c. CYCLIC OXIDATION KINETICS OF DSNiCrAl IN 1.33×10^3 N/m^2 (10 TORR) AIR. THE BOLD LINES INDICATE THE RESULTS AT 1473°K (1200°C). THE LIGHT LINES AT 1373°K (1100°C).

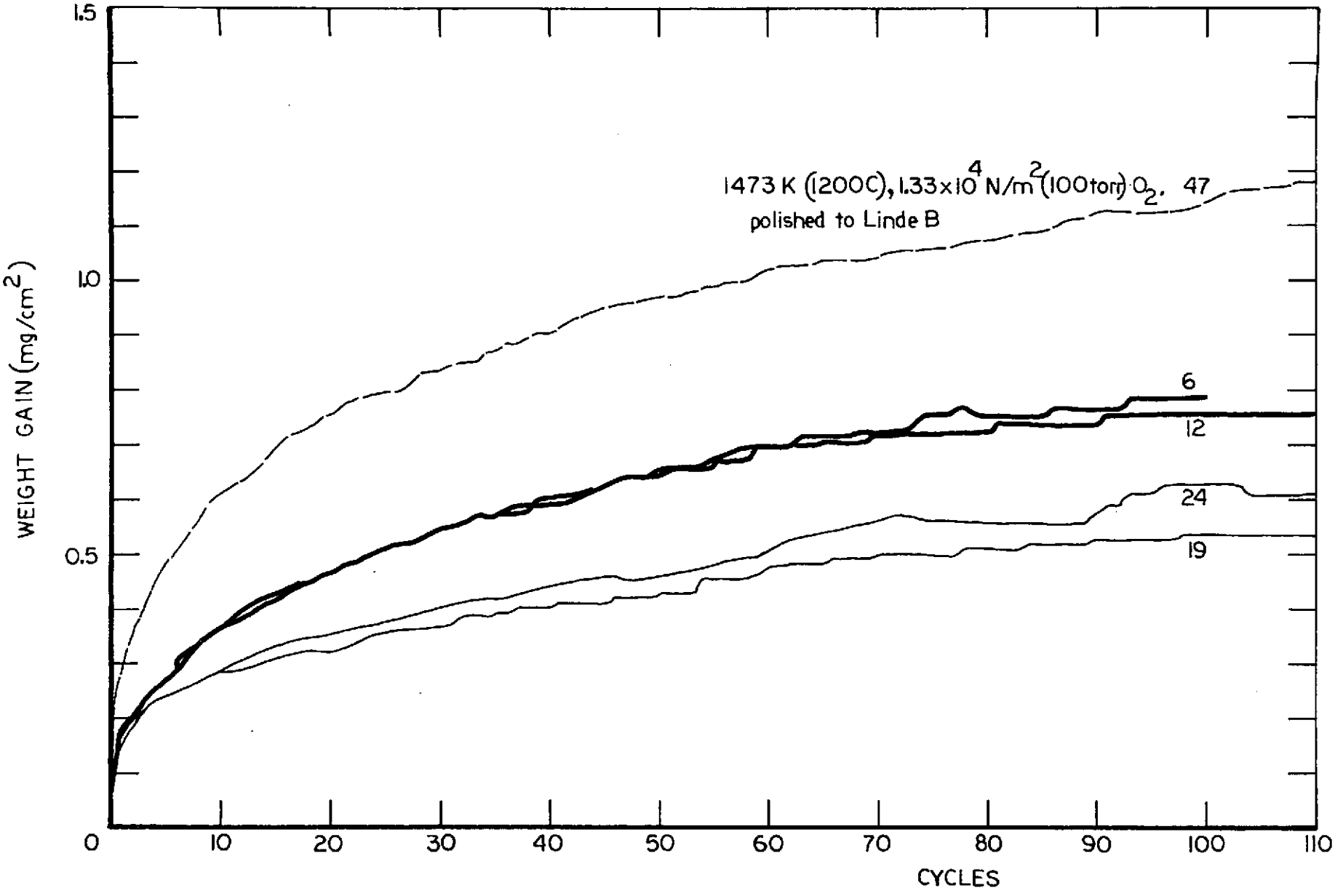

FIGURE 9d. CYCLIC OXIDATION KINETICS OF DSNiCrAl IN 1.01 x 10^5 N/m^2 (760 TORR) AIR. THE BOLD, FULL LINES INDICATE THE RESULTS AT 1473°K (1200°C), THE LIGHT, FULL LINES AT 1373°K (1100°C).

TABLE 7. SUMMARY OF PARABOLIC RATE CONSTANTS FOR OXIDATION OF DSNiCrAl

Temperature,		Air Pressure,		Initial kp	Final kp
^oK	^oC	N/m^2	torr	$(kg^2/m^4.s)$	$(kg^2/m^4.s)$
1373	1100	1.33×10^3	10	1.3×10^{-10}	1.4×10^{-10}
1373	1100	1.33×10^4	100(A)	--	--
1373	1100	1.01×10^5	760	6.4×10^{-10}(B)	--
1473	1200	1.33×10^3	10	8.0×10^{-9}	4.1×10^{-10}
1473	1200	1.33×10^4	100(A)	1.7×10^{-9}(B)	--
1473	1200	1.01×10^5	760	7.9×10^{-10}	1.5×10^{-10}

(A) Oxygen
(B) Surface polished on 3×10^{-8}m paste.

A change in surface finish of DSNiCrAl from surface ground (as-received) to polished (on 3×10^{-8}m paste) led to larger initial rates of oxidation (Figures 9a, 9b, and 9d). From the known effects of alloy grain size, surface finish and oxide internuclear spacing on the rate of establishment of the thermodynamically most stable oxide, this effect was probably associated with an extension of the period of transient oxidation and the consequent formation of amounts of NiO, $Ni(Cr,Al)_2O_4$, and Cr_2O_3 before the rate-controlling basal layer of α - Al_2O_3 became complete. Kear et al[11] have observed the production of this sequence of oxides during the transient oxidation of a dispersion-free Ni-15%Cr-6%Al alloy.

After 3.6×10^4 to 5.4×10^4 s (10 to 15 h) oxidation, the polished specimens oxidized at essentially the same rate as surface ground coupons, as expected. In addition the effect of surface finish was more pronounced at 1.01×10^5 N/m^2 (760 torr) than 1.33×10^3 N/m^2 (10 torr) air.

2. Thickness Change Measurements. An attempt has been made to assess the rate of oxidation by measuring the extent of metal recession, and some results are given in Table 8. Oxidized coupons were mounted in epoxy next to a piece of the same coupon which had been removed prior to oxidation, care being taken to align the coupons normal to the face of the mount. Measurements were made of the thickness at 25 points along each coupon, before and after oxidation, from micrographs of the entire cross section taken at 200X. The maximum error from all sources in this method was estimated to be approximately 1×10^{-5} m. Since the change in thickness of the coupons and the standard deviation of the measurements on an individual coupon were also of this order, it is concluded that this method is unsuitable for measuring the oxidation rate of this alloy.

TABLE 8. CHANGE IN THICKNESS OF DSNiCrAl AFTER OXIDATION (ALL THICKNESSES IN μm)

Specimen Number	Oxidation Treatment	Unexposed Mean Thickness, $\bar{t}$	Unexposed Standard Deviation, σ	Exposed $\bar{t}$	Exposed σ	Δt
20	1.84×10^5s (51 h), 1373°K, 1.33×10^3 N/m^2 (10 torr) air	276.5	2.2	270.5	2.9	6.0
11	1.8×10^5s (50 h), 1473°K, 1.33×10^3 N/m^2 (10 torr) air	260.5	6.7	256	7.6	4.5
21	2.0×10^5s (55.5 h) cyclic to 1473°K (1200°C), 1.33×10^3 N/m^2 (10 torr) air	291	3.7	282	2.6	9.0
5	1.84×10^5s (51 h), 1473°K, 1.01×10^5 N/m^2 (760 torr) air	276	2.5	270.5	2.9	6.0
6	1.8×10^5s (50 h), cyclic to 1473°K (1200°C), 1.01×10^5 N/m^2 (760 torr) air	255.5	6.5	244.8	7.3	10.7

3. Kinetics of Doped DSNiCrAl Alloys. The doped alloys produced by pack-annealing treatments 1 and 2 were oxidized to form an oxide scale suitable for emittance testing, and the alloy from treatment 3 was oxidized to determine any effect of the dopant on the oxidation resistance of DSNiCrAl. Details of these oxidation tests are given in Table 9.

Ideally, in order to introduce a maximum of dopant into the scale, the conditions of oxidation should be chosen to maximize the amount of transient oxides formed, since it is generally understood that impurity elements do not enter chromia or alumina scales in any amounts once these have become established. In the confines of this program, such conditions would be high temperature, high oxygen pressure, and a polished surface finish, that is, 1473°K (1200°C), 1.01×10^5 N/m^2 (760 torr) air, with the coupons polished to Linde B. However, because of an occasional instability in the signal from the oxidation microbalance when operated at 1.01×10^5 N/m^2 (760 torr) which hinders discrimination between similar oxidation rates, the oxidation conditions chosen for the coupons from treatment 1 were 1473°K (1200°C), 1.33×10^3 N/m^2 (10 torr) air, and a Linde B surface finish. Some coupons were abraded to 240 grit to approximate the finish of the as-received sheet. One coupon of each alloy was also oxidized as-pack annealed, and one as-preoxidized and pack annealed.

In general, the isothermal or cyclic kinetics of the coupons from treatment 1 which were metallographically ground before oxidation to remove

TABLE 9a. OXIDATION TEST DATA FOR DOPED DS NiCrAl (BATCH 1)
ALL TESTS AT 1473°K (1200°C) IN 1.33×10^3 N/m^2
(10 TORR) AIR

Alloy	Specimen Number	Exposure Time s	Exposure Time h	Mode*	Weight Change (kg/m^2 x 10^2) Cahn	Weight Change (kg/m^2 x 10^2) Overall	Pretreatment
DS NiCrAl-Mn	13 (A)	1.8×10^5	50	I	1.101	- 0.025	Preoxidized, as pack-annealed.
	14 (AA)	2.29×10^5	63.5	I	0.720	- 0.014	As pack-annealed.
	17 (C)	1.55×10^5	43	I	0.826	0.839	Preoxidized pack-annealed, polished to Linde B.
	18 (CC)	2.34×10^5	65	I	1.02	1.03	Pack-annealed, polished to Linde B.
	31 (D)	1.87×10^5	52	I	0.844	0.844	Preoxidized, pack-annealed, polished to 240 grit.
	32 (DD)	1.98×10^5	55	C	-	0.880	Pack-annealed, polished to 240 grit.
DS NiCrAl-Co	15 (E)	1.84×10^5	51	I	0.966	0.900	Preoxidized, as pack-annealed.
	16 (EE)	1.8×10^5	50	I	0.480	0.470	As pack-annealed.
	33 (G)	2.02×10^5	56	C	1.024	1.070	Preoxidized, pack-annealed, polished to Linde B.
	34 (GG)	1.84×10^5	51	I	0.956	0.965	Pack-annealed, polished to Linde B.
	35 (H)	1.84×10^5	51	I	0.588	0.660	Preoxidized, pack-annealed, polished to Linde B.
	36 (HH)	1.76×10^5	49	C	1.097	1.125	Pack-annealed, polished to Linde B.
DS NiCrAl-Fe	36 (I)	2.03×10^5	56.5	C	0.017	- 0.147	Preoxidized, as pack annealed.
	38 (II)	1.87×10^5	52	I	0.738	0.141	As pack annealed.
	39 (J)	2.61×10^5	72.5	I	0.736	0.586	Preoxidized, pack annealed, polished to 240 grit.
	40 (JJ)	2.47×10^5	68.5	C	0.377	0.214	Pack-annealed, polished to 240 grit.
	41 (L)	1.98×10^5	55	C	1.015	1.01	Preoxidized, pack-annealed, polished to Linde B.
	42 (LL)	2.52×10^5	70	I	0.952	1.01	Pack annealed, polished to Linde B.

* I = isothermal; C = cyclic.
One cycle ≡ 1.8×10^3 s at temperature.

TABLE 9b. OXIDATION TEST DATA FOR DOPED DSNiCrAl (BATCH 2)

(All tests at 1473°K (1200°C), 1.01×10^5 N/m^2 (760 torr) air.)

Specimen No.	Exposure Time s	Exposure Time h	Mode*	Weight Change ($kg/m^2 \times 10^2$) Cahn	Weight Change ($kg/m^2 \times 10^2$) Overall	Pretreatment
DSNiCrAl-Mn						
55	2.20×10^5	61	I	1.054	--	Pack annealed, polished to 6×10^{-6}m finish
57	1.8×10^5	50	I	0.931	0.244	Pack annealed, polished to 600 grit
60	2.54×10^5	71.5	C	0.984	0.770	Pack annealed, polished to 600 grit
DSNiCrAl-Co						
53	2.26×10^5	62.7	I	1.283	0.568	Pack annealed
56	2.7×10^3	0.75	I	0.159	0.188	Pack annealed, polished to 6×10^{-6} m finish
58	2.22×10^5	61.7	I	1.017	0.990	Pack annealed, polished to 600 grit
59	1.78×10^5	49.5	C	0.984	0.976	Pack annealed, polished to 600 grit

*I = isothermal
C = cyclic, one cycle ≡ 1.8×10^3s at temperature

TABLE 9c. OXIDATION TEST DATA FOR Mn-DOPED DSNiCrAl (BATCH 3)

Specimen No.	Temperature		Air Pressure		Time		Weight Change (kg/m^2 x10^2)		Rate Index	Initial kp** ($kg^2/m^4.s$)	Final kp** ($kg^2/m^4.s$)
	°K	°C	N/m^2	torr	s	h	Cahn	Overall	n**		
106	1373	1100	$1.33x10^3$	10	$1.8x10^5$	50	0.318	0.270	3.1	--	--
70	1373	1100	$1.33x10^3$	10	$1.84x10^5$	51	0.468	0.447	4.3 to 3.0	--	--
67	1373	1100	$1.33x10^3$	10	$1.82x10^5$	50.5C*	0.469	0.524	--	--	--
68	1373	1100	$1.33x10^3$	10	$1.78x10^5$	49.5C	0.571	0.537	--	--	--
91	1373	1100	$1.01x10^5$	760	$1.82x10^5$	50.5	0.319	0.232	4.5	--	--
93	1373	1100	$1.01x10^5$	760	$1.84x10^5$	51	0.276	0.285	3.3	--	--
104	1373	1100	$1.01x10^5$	760	$1.84x10^5$	51C	0.546	0.511	--	--	--
105	1373	1100	$1.01x10^5$	760	$2.18x10^5$	60.5C	0.515	0.499	--	--	--
71	1473	1200	$1.33x10^3$	10	$1.8x10^5$	50	0.865	0.975	2.3	$6.5x10^{-10}$ ($0-4.32x10^4$s)	$3.2x10^{-10}$ ($4.32x10^4$-$1.8x10^5$s)
88	1473	1200	$1.33x10^3$	10	$1.82x10^5$	50.5	0.740	0.737	1.4 to 2.3	$4.4x10^{-10}$ ($0-3.6x10^4$s)	--
94	1473	1200	$1.33x10^3$	10	$1.89x10^5$	52.5	0.969	0.035	3.0	--	--
95	1473	1200	$1.33x10^3$	10	$1.73x10^5$	48C	0.934	0.943	--	--	--
96	1473	1200	$1.33x10^3$	10	$1.82x10^5$	50.5C	0.969	0.995	--	--	--
97	1473	1200	$1.01x10^5$	760	$1.8x10^5$	50	0.942	0.752	2.1 to 2.6	$1.3x10^{-9}$ ($0-3.6x10^3$s)	--
89	1473	1200	$1.01x10^5$	760	$1.8x10^5$	50	0.901	0.984	1.4 to 2.3	--	$3.9x10^{-10}$ ($5.4x10^4$-$1.8x10^5$s)
90	1473	1200	$1.01x10^5$	760	$1.84x10^5$	51	0.985	0.924	3.4	--	--
92	1473	1200	$1.01x10^5$	760	$1.75x10^5$	48.5C	0.895	0.308	--	--	--
98	1473	1200	$1.01x10^5$	760	$1.82x10^5$	50.5C	0.923	0.714	--	--	--
99	1473	1200	$1.01x10^5$	760	$1.78x10^5$	49.5C	0.863	0.900	--	--	--

* Cyclic oxidation test, 1 cycle = $1.8x10^3$s

** From $w^n = k.t$ relationship. For parabolic oxidation, n = 2.0, k = kp.

adherent pack alloy were little different from those of the undoped alloy, and were not greatly affected by differences in surface finish. Exceptions to this behavior were probably related to the extent of scale spallation at temperature and on cooling. The coupons oxidized in the as-pack annealed and as-preoxidized and pack annealed conditions often oxidized isothermally at a slower rate than the undoped alloy, but, with the exception of the cobalt-containing alloy, underwent extensive scale spallation on cooling from temperature. These differences presumably result from the presence of a layer of pack-alloy on the coupons, which is enriched in aluminum and chromium, but contains no thoria. These data are analyzed in Table 9a. With a few exceptions the isothermal oxidation kinetics of these alloys could be approximated to a parabolic rate law at least over part of the exposure period. The resulting parabolic rate constants were around 3×10^{-10} $kg^2/m^4.s$ initially to 6×10^{-10} $kg^2/m^4.s$ finally (after 3.6×10^4 to 7.2×10^4 s (10-20 h)) irrespective of dopant. These values are similar to those found for the undoped alloy. In a few cases initial rate constants some ten times greater were measured, but these did not correlate with any systematic differences in coupon chemistry or surface finish.

Since metallographic and electron microprobe examination of the coupons from the Batch 2 doping runs indicated that the surfaces were relatively clean and free of adherent pack-alloy, coupons were oxidized with no further surface preparation. Unfortunately, the dark grey scales produced on these coupons spalled extensively on cooling after oxidation. Adherent scales were only successfully produced on these doped coupons after approximately 3.5×10^{-5} m of material was abraded from each side before oxidation. The oxidation conditions finally used, together with the other test data are listed in Table 9b. All the coupons oxidized isothermally or cyclically at rates slightly faster than those determined for the undoped alloy under the same conditions. Parabolic behavior (rate index $\simeq$ 2.0) was only observed for the first 5.4×10^3 to 1.08×10^4 s (1.5 to 3 h) of oxidation, after which the rate index increased towards 3.0. The parabolic rate constant calculated for the initial stages of oxidation was 1.2 to 1.5×10^{-9} $kg^2/m^4.s$ which compares to 1.5 to 7.9×10^{-10} $kg^2/m^4.s$ for the undoped alloy.

A similar surface preparation procedure was adopted for the oxidation test coupons from Batch 3, and 5×10^{-5} m of material was ground off each face using 600 grit paper before oxidation. The results of the extensive oxidation tests on this alloy were reported in Table 9c, and the kinetic curves are shown in Figures 10a to 10d. Curiously, oxidation according to a parabolic rate law was observed only at 1200°C, and then for only 67% of the coupons oxidized. For these, the initial parabolic rate constants are approximately one order of magnitude smaller at 1.33×10^3 N/m^2 (10 torr) pressure and one order of magnitude larger at 1.01×10^5 N/m^2 (760 torr) pressure, than for the undoped alloy (see Table 7), while in the later stage of oxidation the two alloys oxidize at about the same rate.

4. Scale Morphologies. The scales formed on the DSNiCrAl alloy oxidized with a belt-sanded or coarse abraded surface finish were light grey in color, and were tightly adherent to the flat sides of the coupons. Slight spallation occurred along the ridges of grinding grooves, apparently as a result of fluctuations in temperature. In the cyclic oxidation test such spallation may have occurred at temperature, since a number of these test coupons were bent after oxidation, with extensive scale spallation from the concave side, indicating considerable compressive stresses in the scale.

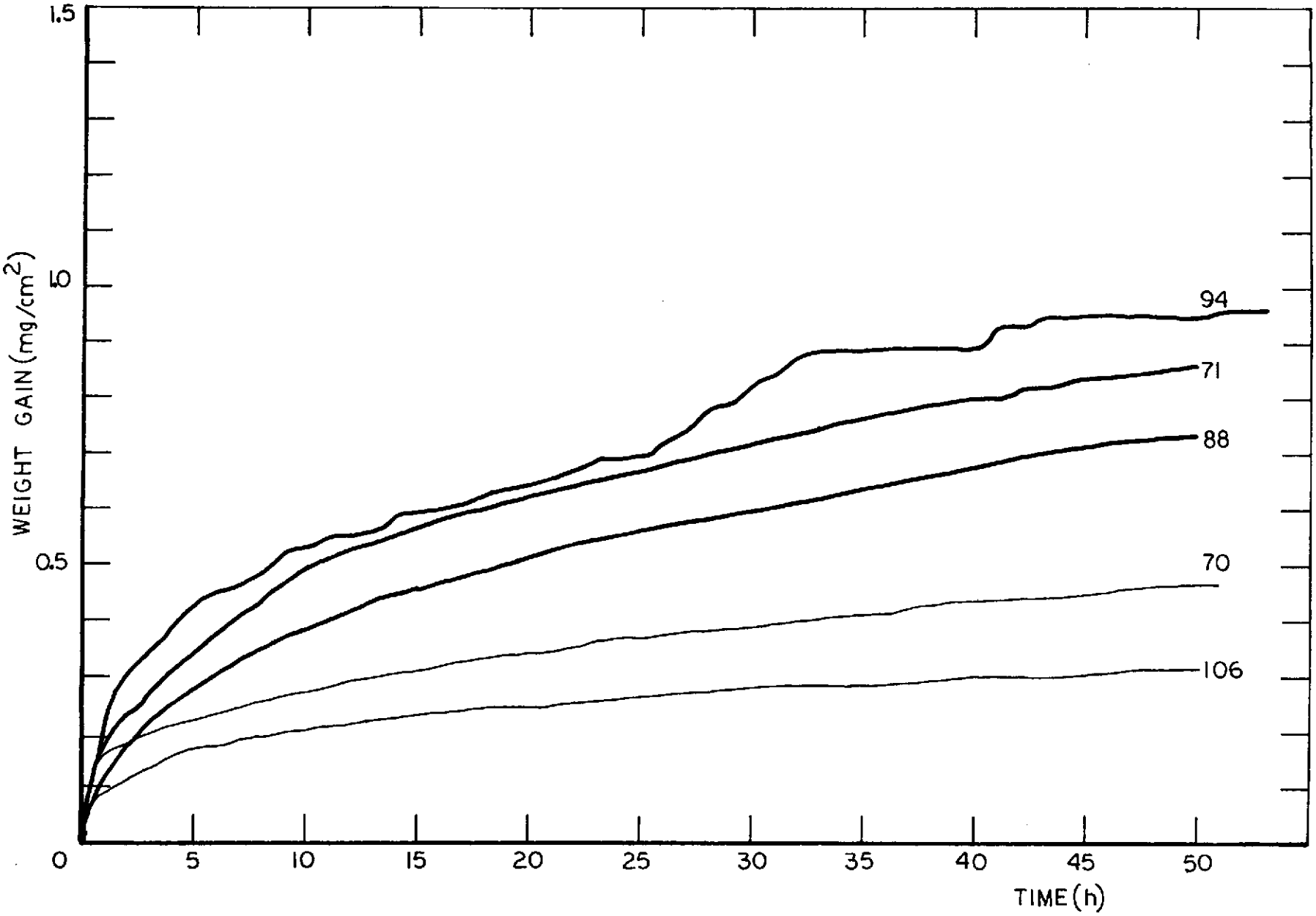

FIGURE 10a. ISOTHERMAL OXIDATION KINETICS OF MANGANESE-DOPED DSNiCrAl (BATCH 3) IN 1.33 x 10^3 N/m^2 (10 torr) AIR. The bold lines indicate results at 1473°K (1200°C), the light lines at 1373°K (1100°C). The numbers on the curves refer to individual coupons, for details see Table 9c.

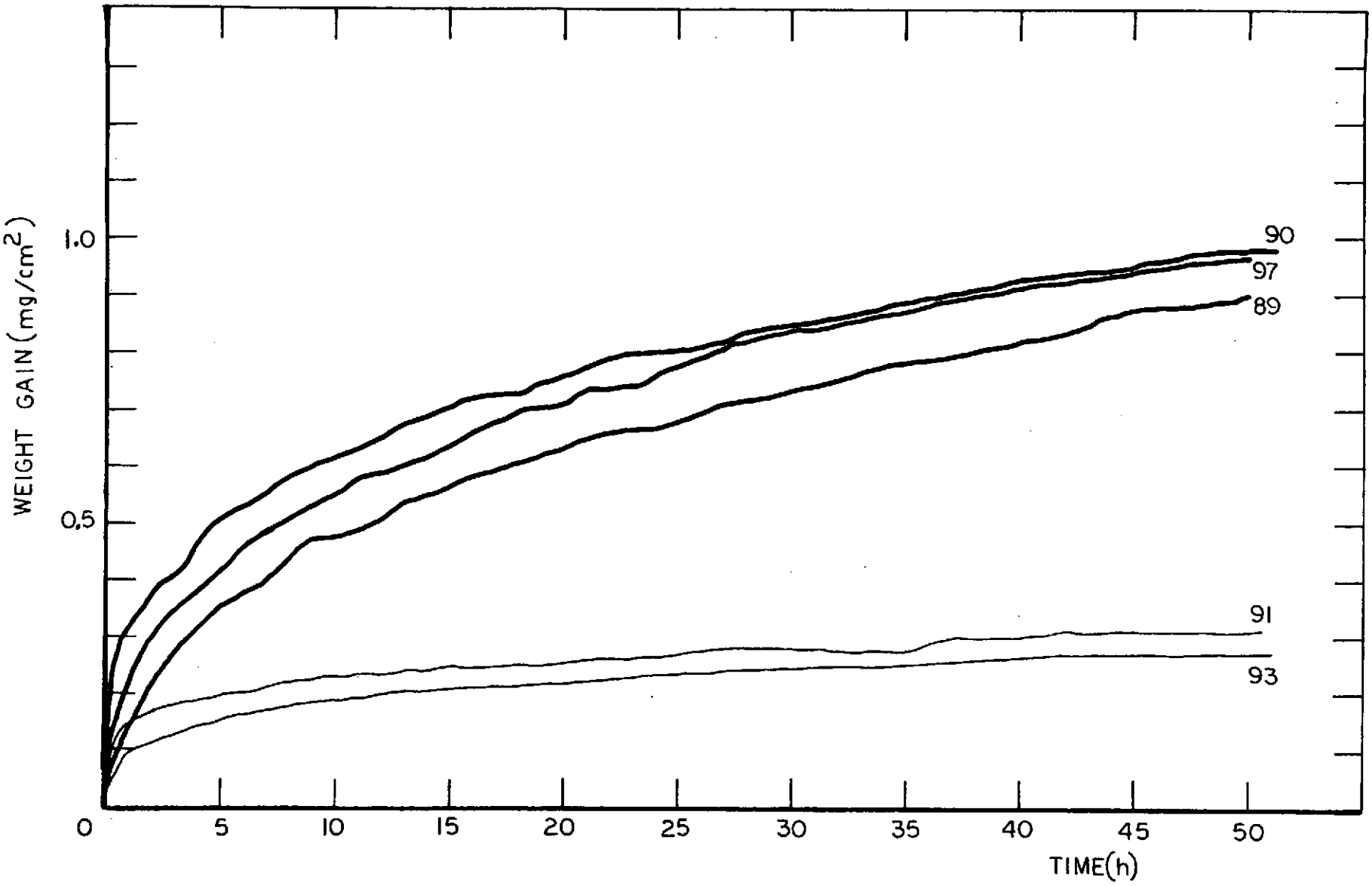

FIGURE 10b. ISOTHERMAL OXIDATION KINETICS OF MANGANESE-DOPED DSNiCrAl (BATCH 3) IN 1.01×10^5 N/m^2 (760 TORR) AIR. The bold lines indicate results at 1473°K (1200°C), the light lines at 1373°K (1100°C).

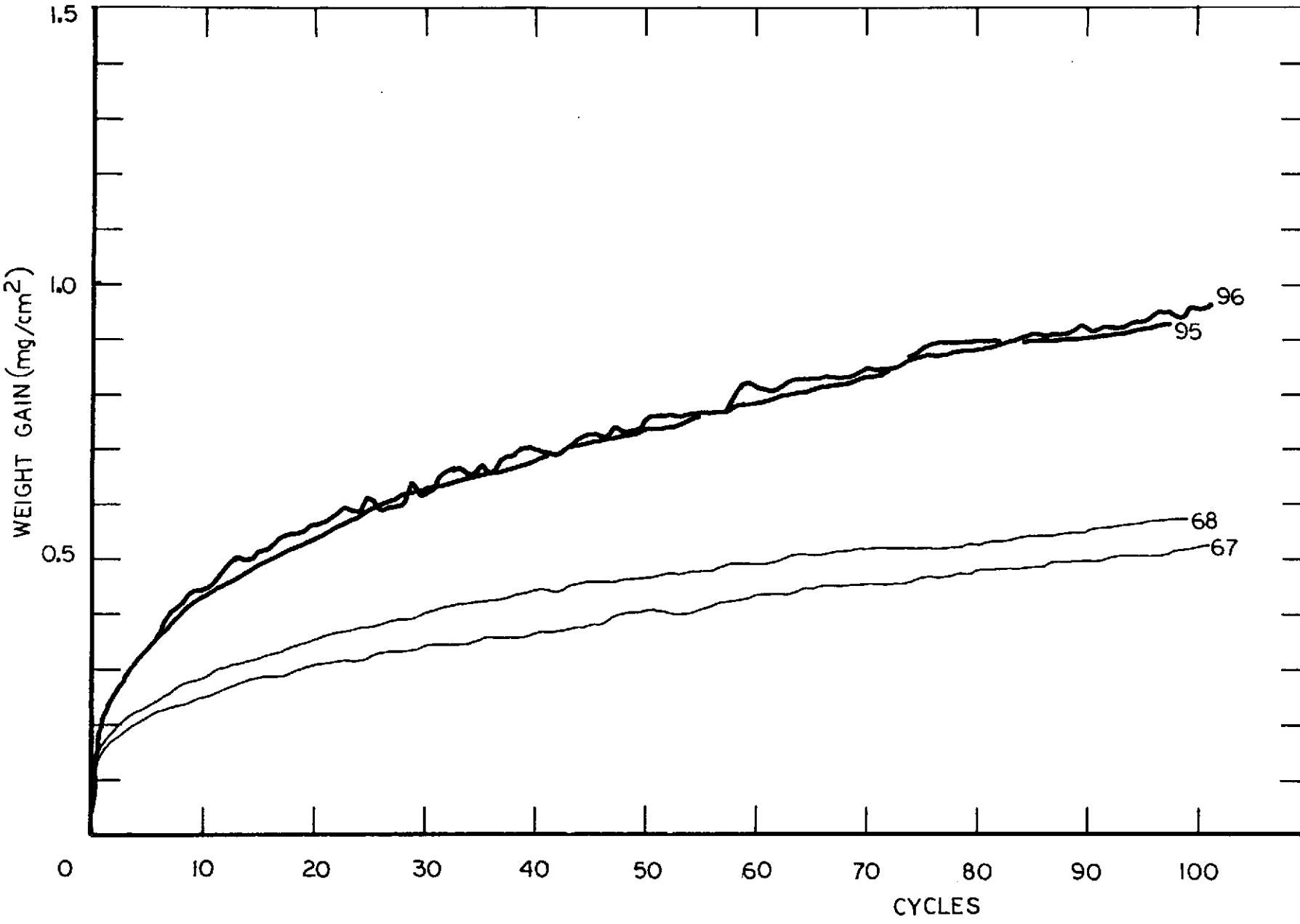

FIGURE 10c. CYCLIC OXIDATION KINETICS OF MANGANESE-DOPED DSNiCrAl (BATCH 3) IN 1.33×10^3 N/m^2 (10 torr) AIR. The bold lines indicate results at 1473°K (1200°C), the light lines at 1373°K (1100°C).

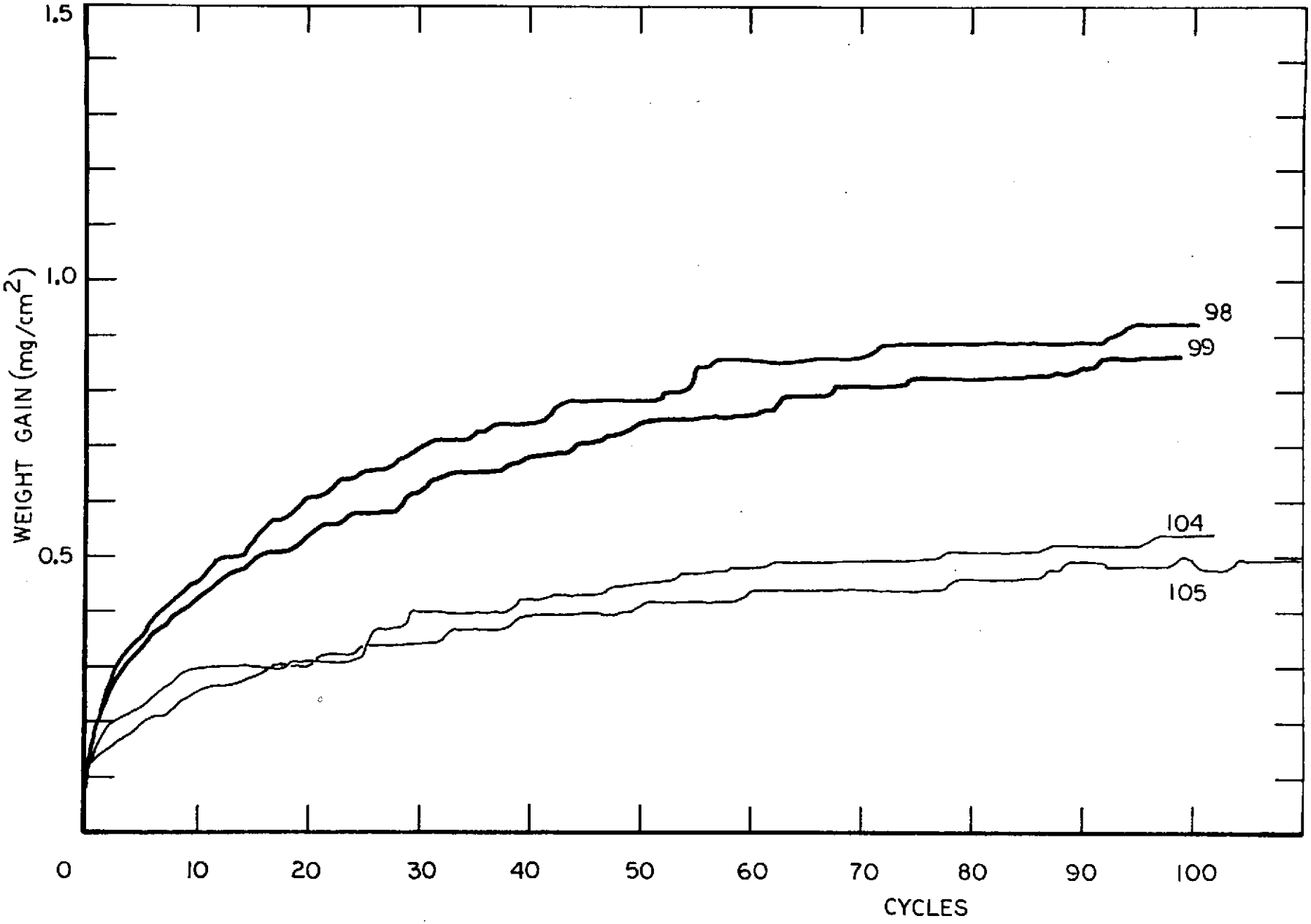

FIGURE 10d. CYCLIC OXIDATION KINETICS OF MANGANESE-DOPED DSNiCrAl (BATCH 3) IN 1.01×10^5 N/m^2 (760 torr) AIR. The bold lines indicate results at 1473°K (1200°C), the light lines at 1373°K (1100°C).

Attempts at detailed topographical examination of the oxides by conventional optical microscopy proved only partially successful; the scales appeared to have very small crystalline features (Figure 11a), but could not be well resolved at magnifications up to 1000 times. Consequently, carbon-platinum replicas were made of the oxide surfaces using a dry-stripping technique[12], and examined in a Siemens Elmiskop IIA electron microscope at 100 KeV. Typical micrographs obtained are shown in Figure 11. The scales have a surface grain size of 0.1 to 0.5 x 10^{-6} m and in some areas clearly defined crystalline features and apparently growth steps are visible (Figure 11f), while in other areas the grains have a rounded appearance (Figure 11e).

Conventional metallographic sections of the scales showed the oxide to be exceptionally uniform in thickness, but often broken into sections and detached from the alloy, especially near irregularities in the alloy surface (Figure 12a). In such areas no evidence of internal oxide formation was found. A more detailed examination of the scale of a specimen oxidized isothermally at 1473°K (1200°C), 1.01 x 10^5 N/m^2 (760 torr) air (Number 1) was made using a Cambridge Stereoscan MK II scanning electron microscope, operated in the secondary electron (SE) mode. The specimen was bent through 1.57 rad to cause some spallation, and the remaining adherent scale was examined in the Stereoscan, after the specimen was first gold-coated. Stereo pairs of micrographs were made of some areas and examined afterwards in a Hilger and Watts SB 180 Mirror Stereoscope.

A typical scanning micrograph of the scale remaining on the alloy surface is shown in Figure 12b, and views at higher magnification are shown in Figures 12c and 12d. The scale is quite uniform in thickness and appears to be columnar-grained and there is possibly a thin outer layer of scale of smaller grain size. The outer scale surface can be seen in Figure 12c to have a grain size smaller than that of the columnar grains in the scale body, and in Figure 12e which is a view at 1.22 rad to the alloy surface, the grain boundaries of the scale surface are recessed, which suggests that some evaporative loss of scale occurred at temperature. The texture of the alloy surface can also be seen in Figure 12e, while Figure 12f shows a piece of scale broken away from the surface and found lying upside down on top of the remaining adherent scale. The underside of this scale has the same texture as the alloy surface, and it appears that each small recession in the alloy surface texture is the imprint of the oxide grain which was growing in that location. The fit of the oxide scale to the alloy surface was obviously very good, even at surface imperfections. Figure 12d shows a shallow crater in the alloy surface which nevertheless is covered by oxide grain imprints. An isolated grain of oxide is also visible in Figure 12d (arrowed) sitting in the alloy surface.

The fractured scale on a similar, oxidized coupon was examined in a Materials Analysis Company scanning electron microscope, using the backscattered electron mode (BSE), which is sensitive to differences in atomic number and so is useful in locating heavy elements such as thorium[13]. Because of certain design features, this instrument is more useful than the Cambridge instrument for BSE examination of fracture surfaces. A general secondary electron mode (SE) view of the detached scale is shown in Figure 13a, and Figure 13b shows the scale cross section, using the BSE mode. The white dots are thoria particles, which are evidently incorporated in the scale and which also lie on the scale surface; the scale/gas interface is indicated by the arrows. Figures 13c and 13d show a small piece of loose scale which was found upturned and lying on the surface of a strip of adherent scale. Here thoria particles can be seen on

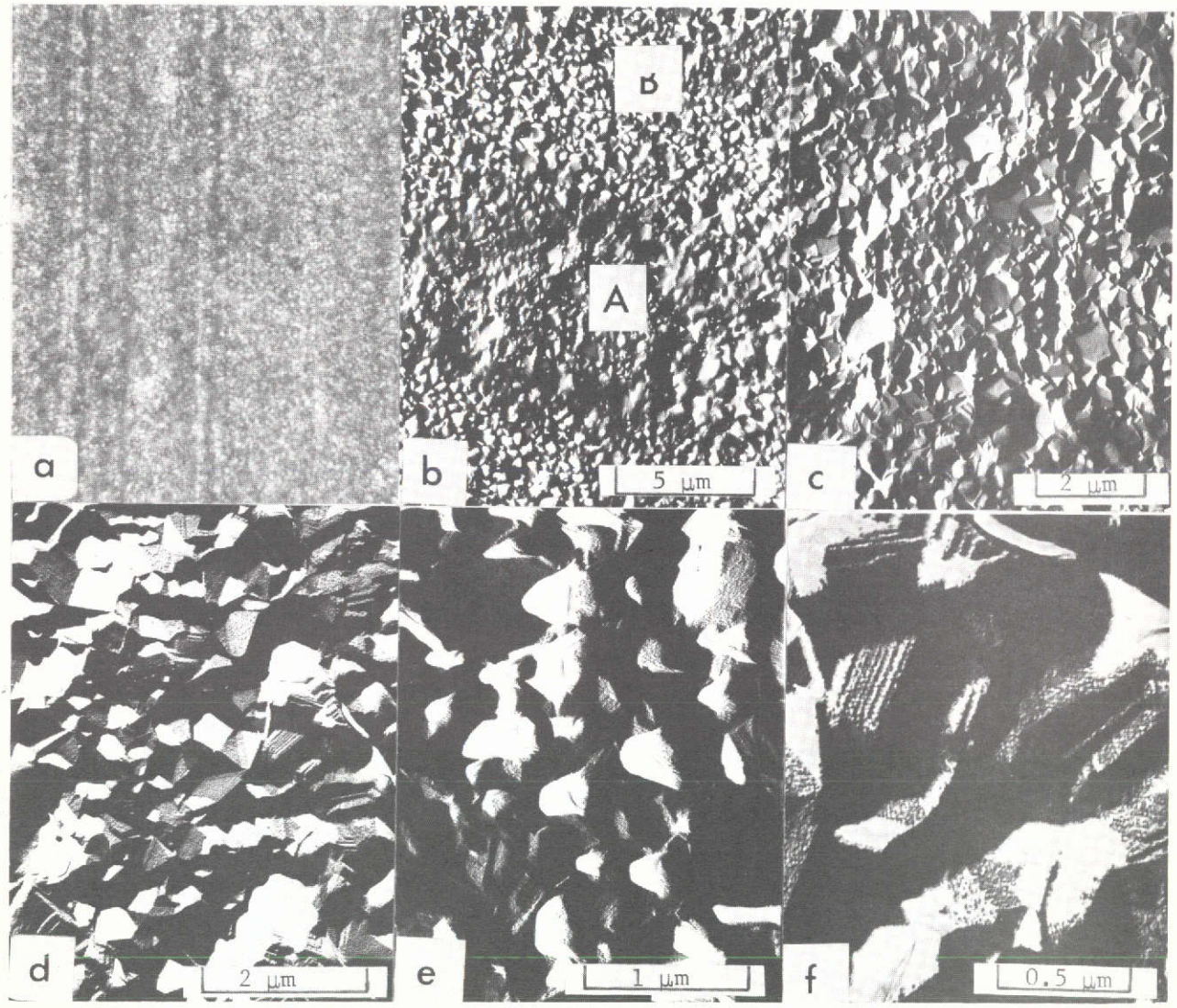

FIGURE 11. TOPOGRAPHICAL FEATURES OF THE SCALE FORMED AFTER 1.8×10^5s (50 HOURS) OF ISOTHERMAL OXIDATION AT 1473°K (1200°C)

(a) Optical micrograph, showing the generally small grain size of the scale, and the scale contours over sanding marks in the alloy surface, X500, bright field (Specimen No. 11).

(b to f) Transmission electron micrographs of carbon/platinum replicas taken from the surface of Specimen No. 1. (b) X4000; (c) X8000 of area A in (b); (d) X12,000 of (c); (e) X24,000 of area B in (b); (f) X38,000 of (d).

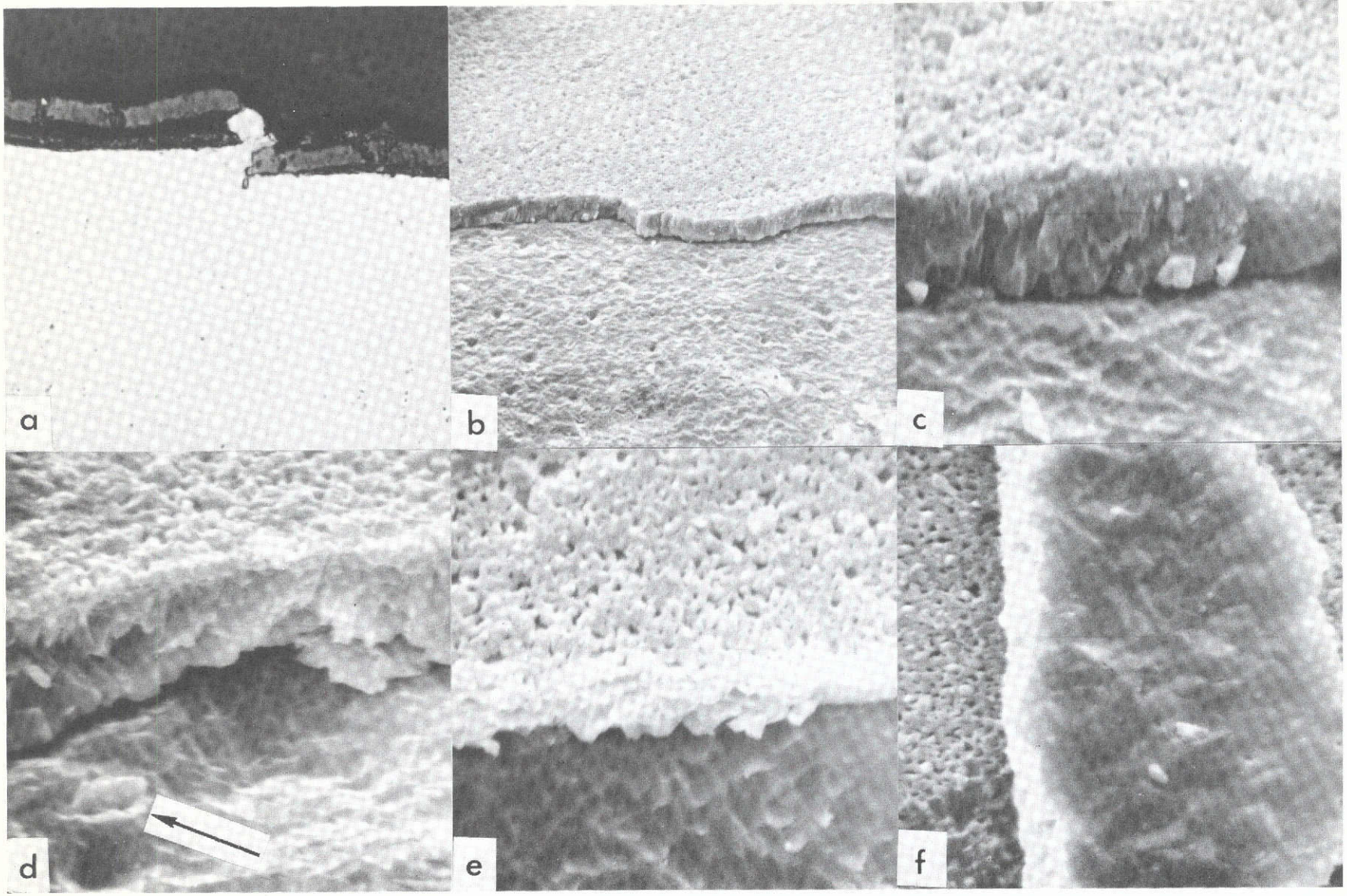

FIGURE 12. SECTIONS OF THE SCALE FORMED ON DSNiCrAl AFTER ISOTHERMAL OXIDATION AT 1473°K (1200°C) FOR 1.8×10^5s (50 HOURS)

(a) Optical micrograph of the scale on Specimen No. 11, X1000; (b to f) scanning electron (SE mode) micrographs of fracture sections of the scale formed on Specimen No. 1. (b) X1000 at 0.61 rad. to the alloy surface; (c and d) X4700 at 0.61 rad.; (e) X4700 at 1.22 rad.; (f) X4700 at 1.29 rad., underside of scale

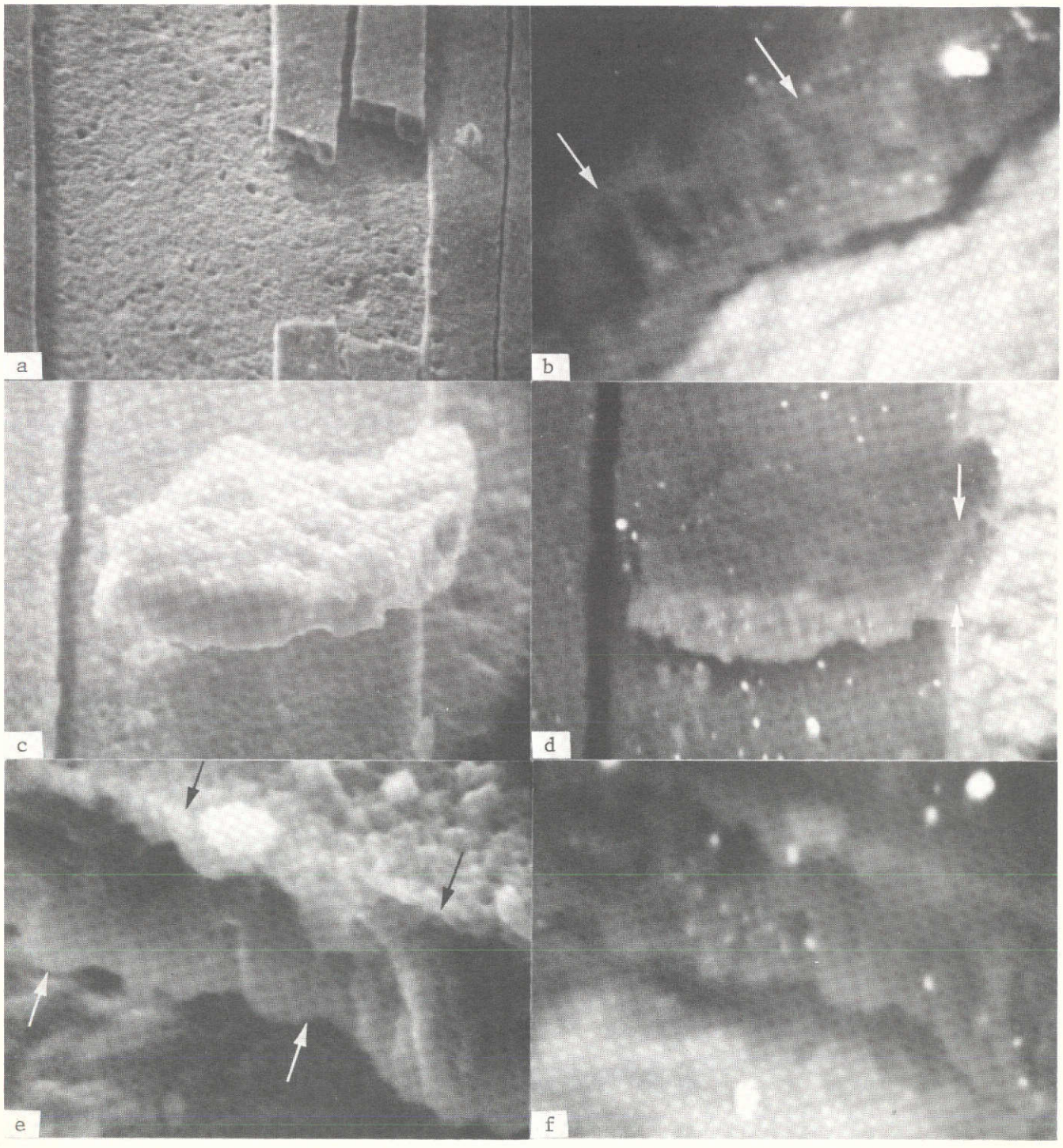

FIGURE 13. FRACTURE SECTIONS OF ALUMINA SCALE FORMED ON DSNiCrAl AFTER CYCLIC OXIDATION FOR 1.8×10^5s (50 HOURS) AT 1473°K (1200°C), 1.01×10^5 N/m^2 (760 TORR) AIR (Specimen No. 2)

(a) General surface view, showing scale fractured into strips, secondary electron mode (SE), X500, at 0.91 rad. to surface.

(b) Close view of fracture section of scale in back-scattered electron mode (BSE), showing thoria particles in scale as white dots. At 0.79 rad. to surface, X5000.

(c) and (d) Complementary SE and BSE images of an upturned piece of scale, at 0.91 rad. to surface, X2000.

(e) and (f) Complementary SE and BSE images of fracture surface of scale at 0.91 rad., X5000.

underside of this cale, on the top side of the adherent scale, and in the scale fracture section (arrowed). Figures 13e and 13f are complementary high-resolution and composition-sensitive views of the fracture section of the scale, which again show thoria particles incorporated, in a not very uniform manner, in the scale. In Figure 13e the white arrows indicate the underside of the scale which has lifted away from the alloy surface, and the black arrows point out the scale/gas interface.

In general, the scales formed on the manganese-doped DSNiCrAl alloy were dark grey, or grey-brown in color, and where all the adherent thoria-free pack alloys had been removed prior to oxidation, were extremely adherent. The topographical features of these scales were difficult to discern because the brown coloration apparently resulted from the presence of a thin, loosely adherent outer layer of manganese-containing oxide. In cross section these scales were hardly distinguishable from these on the undoped alloy (Figure 14a) but in the scanning electron microscope, this thin outer layer was visible and appeared to comprise relatively isolated crystallites (Figures 14b-d). Spot analyses of the crystallites marked in Figure 14c, using an Ortec Model 6200 multichannel analyzer attachment on the Cambridge Stereoscan instrument, indicated intensity ratios for Al:Cr:Ni:Mn of 100:6:3:3 in A and 100:6:5:7 in B. Similar analysis of the cross-section of the bulk of the scale at C gave intensity ratios of 100:3:9:0.7 for the same elements.

The oxides formed on the undoped and doped alloy were examined by X-ray diffraction. Small samples were scraped from the surfaces of the coupons using a tungsten carbide stylus, and Debye-Scherrer photographs were taken. The results listed in Table 10 show spinel patterns for scales which appeared colored to the eye. Of interest is the absence of spinel on the manganese-doped alloy (No. 17-C) from which a brown outer layer had been removed before XRD analysis. The brown layer brushed off similar coupon No. 32-DD gave a strong spinel (possibly $MnAl_2O_4$) pattern, whereas the sample scraped off coupon 18-CC showed an enhanced ThO_2 pattern.

An electron microprobe line scan through an oxidized DSNiCrAl-Mn coupon (No. 95) illustrates a layer of manganese- aluminum- and chromium-containing oxide some 5 to 6 x 10^{-6} m thick on the outside of the main scale (Figure 15). Also shown in this Figure is the flat manganese concentration profile in the alloy, the manganese level being approximately 2%, and a slight enrichment of chromium (2.5%) in the alloy behind the alumina scale.

5. Ion-Probe Microanalysis of DSNiCrAl. A technique was evolved to enable the alumina scales on the DSNiCrAl alloy to be profiled in plan using the Cameca ion microanalyzer. Essentially, a grid-pattern of a suitable element was vapor deposited on the surface of the film to be examined, the grid being such that the raster of the ion beam could be substantially contained in one of the open areas of the grid, while charge accumulation on the oxide under examination was minimized by leakage along the mesh of the grid. The important characteristics of the element used to form the grid pattern are good electrical conductivity and a low sputtering rate in the ion beam. In this case it was convenient to use aluminum.

A preliminary profile obtained for a coupon of DSNiCrAl oxidized for 6 x 10^2 s (0.2 h) at 1473°K (1200°C), 1.01 x 10^5 N/m^2 (760 torr) air is shown

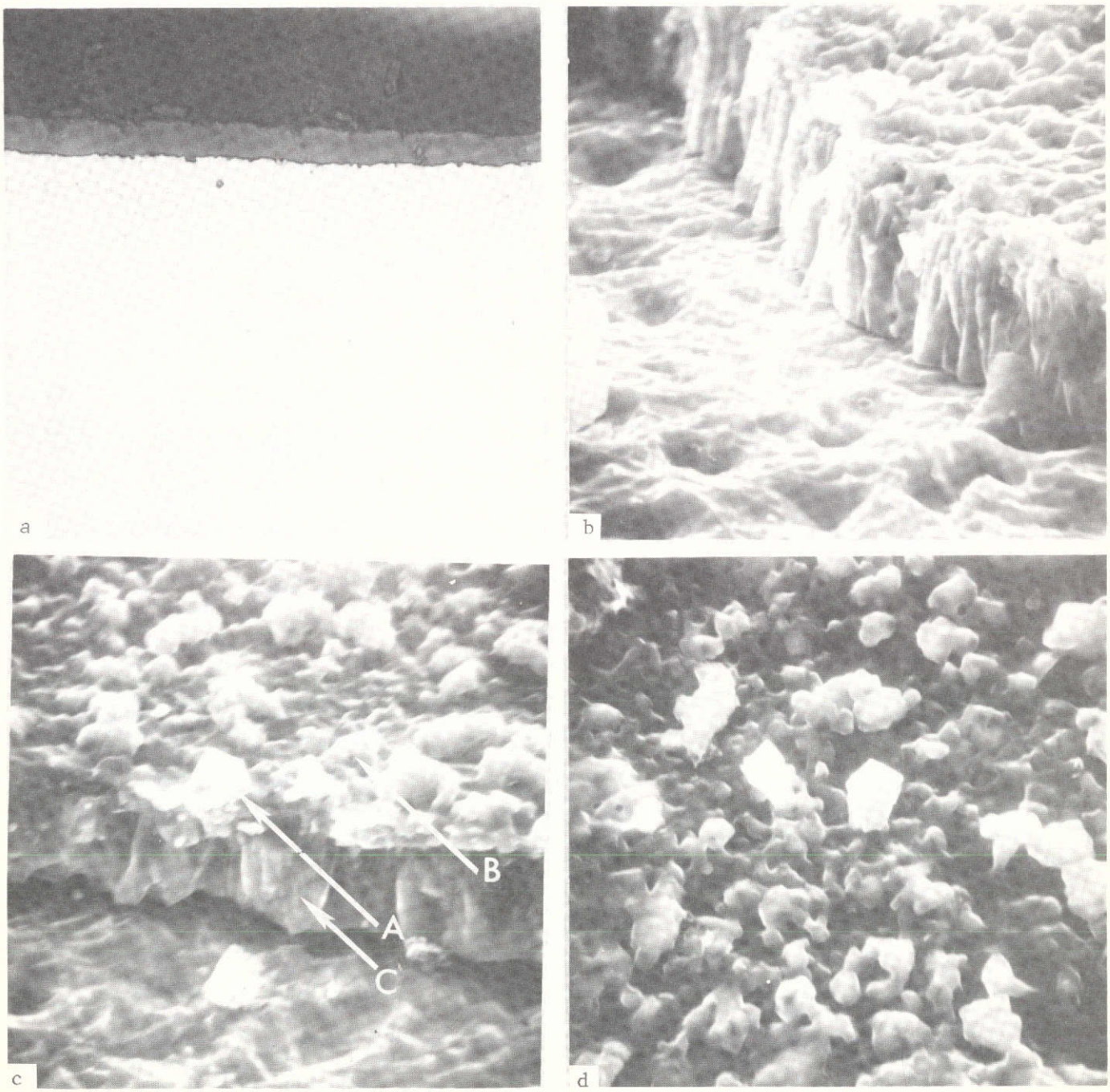

FIGURE 14. SCALES FORMED ON DSNiCrAl-Mn AFTER 1.8×10^5 s (50 h) AT 1473°K (1200°C) IN 1.01×10^5 N/m^2 (760 TORR) AIR

(a) Optical micrograph of scale cross section, X1000 (coupon No. 92), (b) Scanning electron micrograph of fracture cross section of scale, at 1.22 rad. to the alloy surface, X5000 (No. 97), (c) Similar view, at 0.87 rad., X5000 (No. 97), and (d) Outer surface of scale at 0.40 rad., X5000 (No. 97).

TABLE 10. X-RAY DIFFRACTION ANALYSES OF SCALES ON DSNiCrAl ALLOYS

Alloy	Specimen Number	Pretreatment	Oxidation* Mode	Scale Type
DS NiCrAl	4	As-received	I	α-Al_2O_3 > ThO_2, spinel (a_o $\simeq$ 8.09, possibly $NiAl_2O_4$)**
DS NiCrAl	7	As-received	I	α-Al_2O_3 >> ThO_2 > γ(matrix)
DS NiCrAl	29	Polished to Linde B	I	α-Al_2O_3 > ThO_2, spinel (a_o $\simeq$ 8.07, possibly $NiAl_2O_4$)
DS NiCrAl-Mn	17-C	Preoxidized, pack annealed, polished to Linde B	I	α-Al_2O_3, γ(matrix) >> ThO_2
DS NiCrAl-Mn	18-CC	Pack annealed, polished to Linde B	I	α-Al_2O_3 > ThO_2 > spinel (a_o $\simeq$ 8.26, possibly $MnAl_2O_4$)
DS NiCrAl-Mn	32-DD	Pack annealed, polished to 240 grit	C	α-Al_2O_3, spinel ($a_o \simeq 8.27$, possibly $MnAl_2O_4$) > ThO_2
DS NiCrAl-Co	35-H	Preoxidized, pack annealed, polished to Linde B	I	α-Al_2O_3, spinel ($a_o \simeq 8.05$, possibly $NiAl_2O_4$) > ThO_2

* I = isothermal; C = cyclic.

** Lattice parameters (a_o) of possible oxides are:

$NiAl_2O_4$	8.048
$MnAl_2O_4$	8.258
$NiCr_2O_4$	8.32
$NiCrMnO_4$	8.32

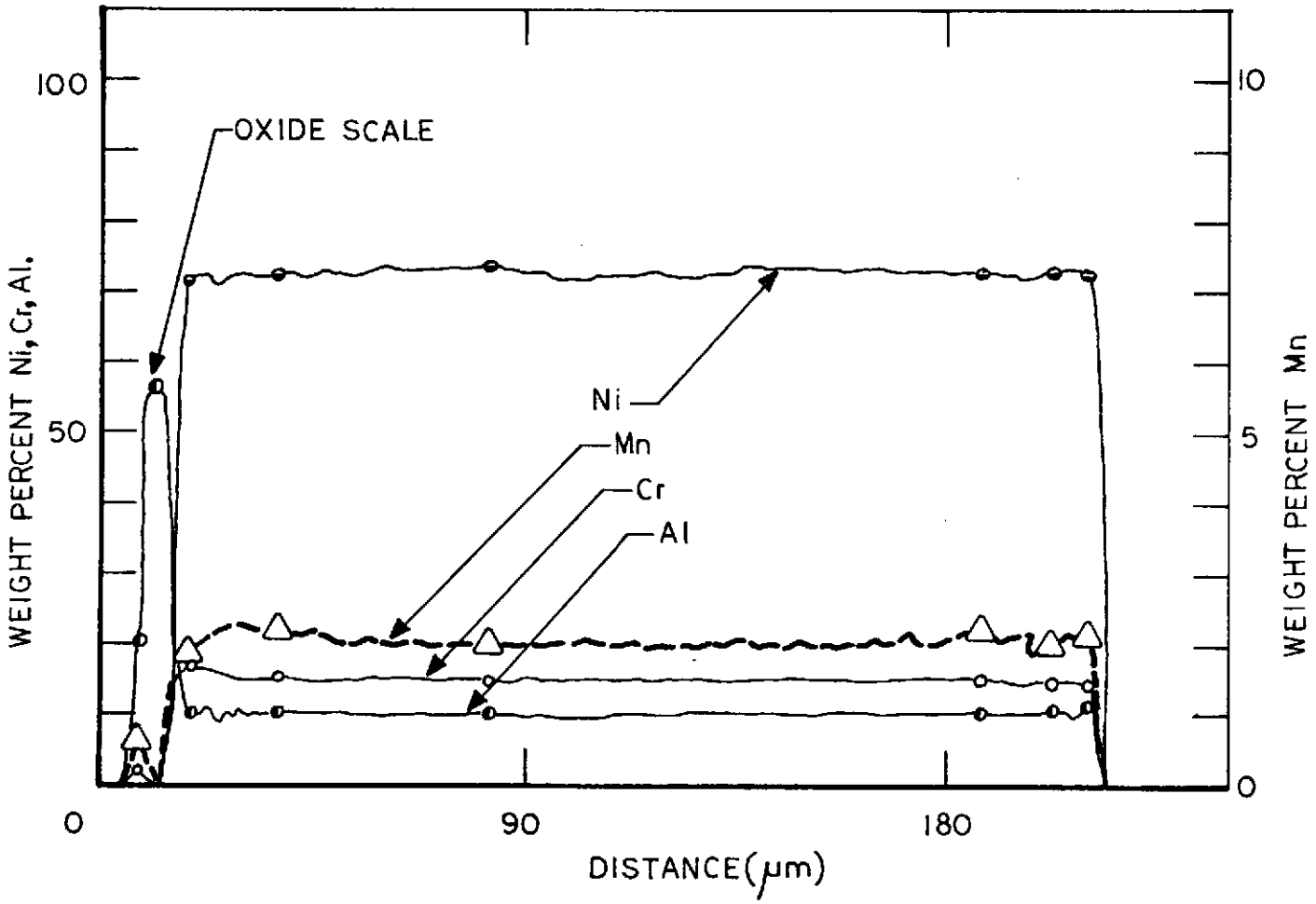

FIGURE 15. CONCENTRATION PROFILE THROUGH DSNiCrAl-Mn$_3$ (BATCH 3) AFTER CYCLIC OXIDATION AT 1473°K (1200°C) IN 1.33 x 10^3 N/m^2 (10 TORR) AIR FOR 1.73 x 10^5 s(48 h) (COUPON NO. 95). The oxide scale was grey/brown in color, and spalled from one side of the coupon on final cooling.

in Figure 16a. Negatively-charged oxygen ions were used at an accelerating voltage of 11 kV. Because the coupon (No. 46) was oxidized with the rough, as-received surface finish, the metal/oxide interface was not sharply defined in the ion microanalyzer, so that no attempt has been made to indicate its location, or to quantify distance in Figure 16a. However, the concentration profiles obtained indicate that thoria is present throughout the scale thickness and that nickel and manganese (present in the alloy as a tramp element) concentrations in the scale are greatest at the scale/gas interface, and decrease in a uniform manner to the scale/metal interface. The chromium profiles show little change in concentration across the thickness of the scale and give no indication of the location of the scale/metal interface. This might be interpreted to mean that the alumina scale contains Cr_2O_3 in solid solution (Cr_2O_3 and α-Al_2O_3 have unlimited solid solubility), although X-ray diffraction of similar scales did not indicate the presence of Cr_2O_3.

Similar profiles through the scales on DSNiCrAl, DSNiCrAl-Mn and DSNiCrAl-Co, polished and oxidized 6.0×10^2 s (0.2 h) at 1473°K (1200°C) in 1.01×10^5 N/m^2 (760 torr) air, are shown in Figures 16b to 16d. An attempt to electropolish the surfaces of these alloys before oxidation, to provide a sharply defined metal/oxide interface, was only successful in the case of the undoped alloy. Consequently the Mn- and Co-containing alloys were oxidized with surfaces which had been carefully polished on 3×10^{-8} m alumina paste on a metallographic wheel.

Concentration profiles are shown in Figures 16b through 16d for chromium, nickel, thorium, and for manganese, iron and cobalt where these could be detected. Because of uncertainties in measuring the oxide thickness, the distance axis in these Figures has been left in arbitrary units. No aluminum profiles were measured since the oxidized specimens were precoated with a conducting aluminum grid, although the profile of the Cr^+_{54} species might contain a contribution from aluminum (via 2x Al^+_{27}).

Despite the precautions, some charge accumulation occurred on the samples causing, in the cases in Figures 16c and 16d, a slight shift in the mass scale which is reflected in the profiles as a downward drift of all the signals. The results in Figure 16b, however, are considered to be relatively free from charge effects and, in the case of the profiles for nickel, iron, manganese, and thorium, are remarkably similar to concentration profiles measured through thin chromia scales formed on TDNiCr[14].

The main features of these results for alumina scales are that manganese and iron (which are present in undoped DSNiCrAl as impurities) as well as nickel and chromium are detected throughout the scale thickness and all except chromium reach a maximum concentration at the oxide/gas interface. The chromium content of the scale reaches a maximum at about a third of the scale thickness from the oxide/gas interface and then decreases sharply towards the oxide/metal interface. The thorium concentration is apparently quite uniform through the scale and probably results from the detection of individual particles of thoria which appeared from scanning electron microscopy to be incorporated throughout the scale thickness.

If the increased tail-off with depth of penetration of the signals in Figures 16c and 16d is a result of charge up of the specimen, then these profiles

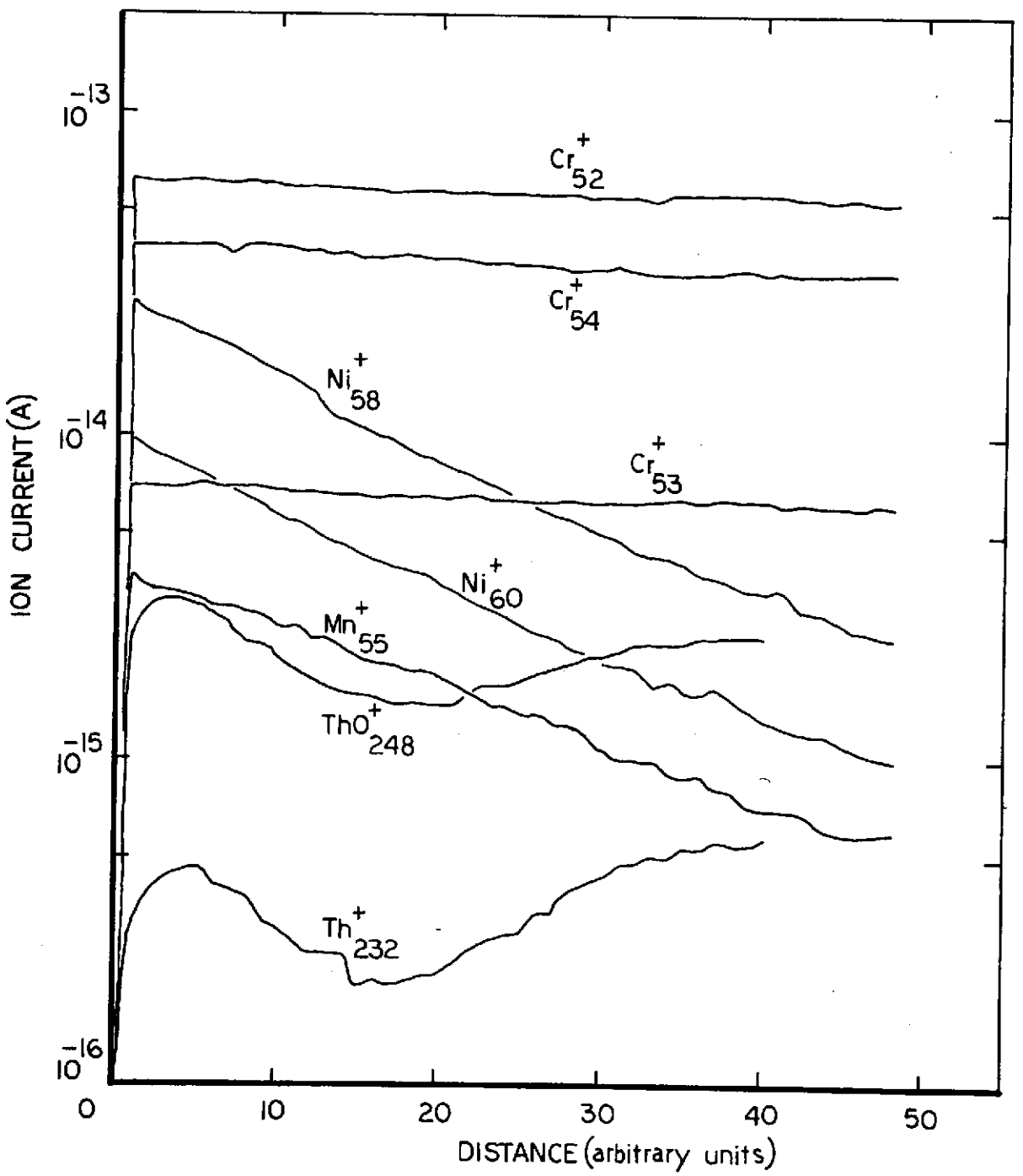

FIGURE 16a. CONCENTRATION PROFILE THROUGH ALUMINA SCALE FORMED ON DSNiCrAl AFTER 6×10^2s (10 min.) AT 1473°K, (1200°C) 1.01×10^5 N/m^2 (760 torr) AIR, BY ION-PROBE MICROANALYZER

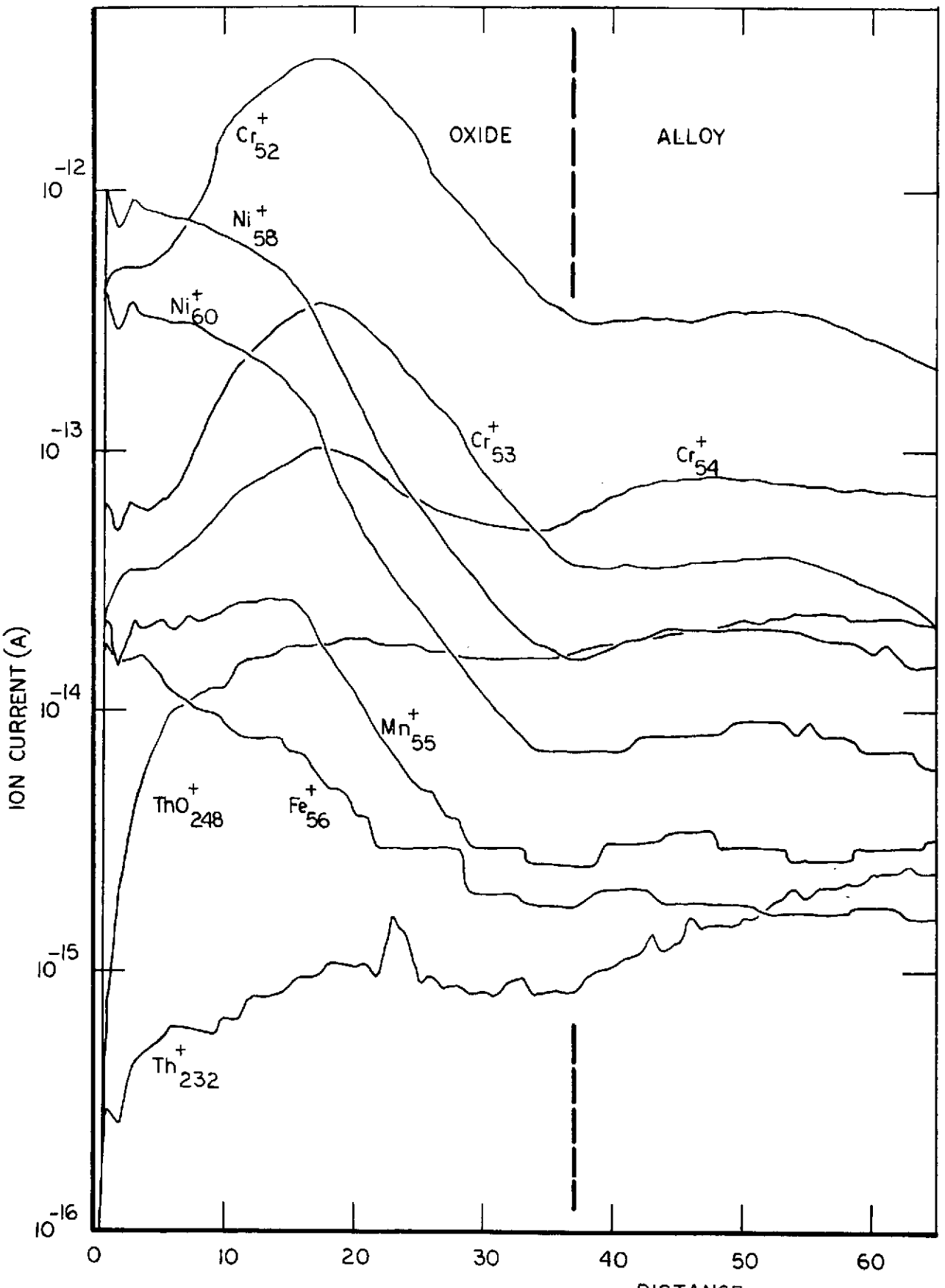

FIGURE 16b. CONCENTRATION PROFILE THROUGH OXIDE SCALE FORMED ON DSNiCrAl AFTER 6 x 10^2s (10 min.) AT 1473°K, (1200°C) 1.01 x 10^5 N/m^2 (760 torr) AIR (No. 63).

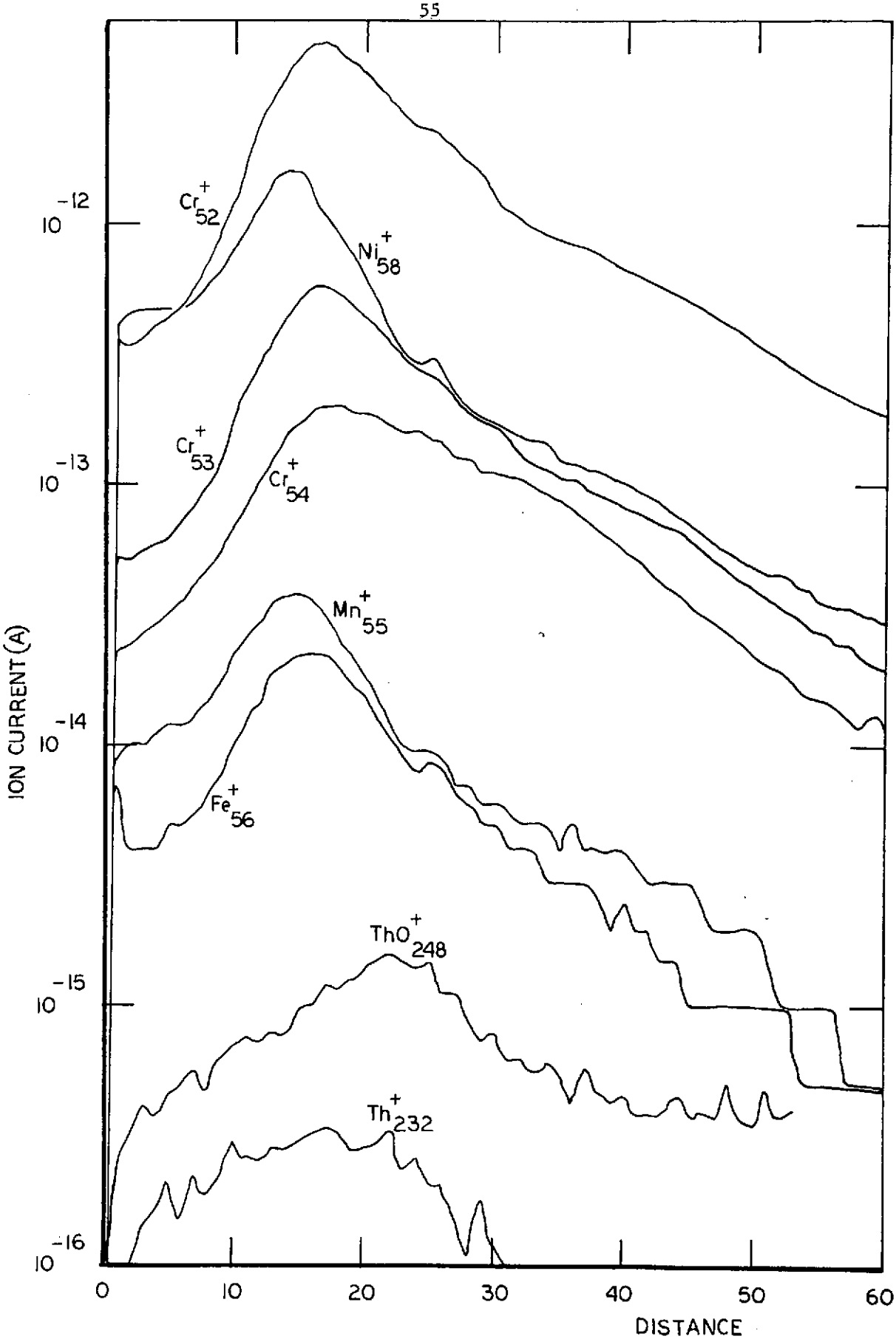

FIGURE 16c. CONCENTRATION PROFILE THROUGH OXIDE SCALE FORMED ON DSNiCrAl-Co AFTER 6 x 10^2s (10 min.) AT 1473°K, (1200°C) 1.01 x 10^5 N/m^2 (760 torr) AIR (No. 64)

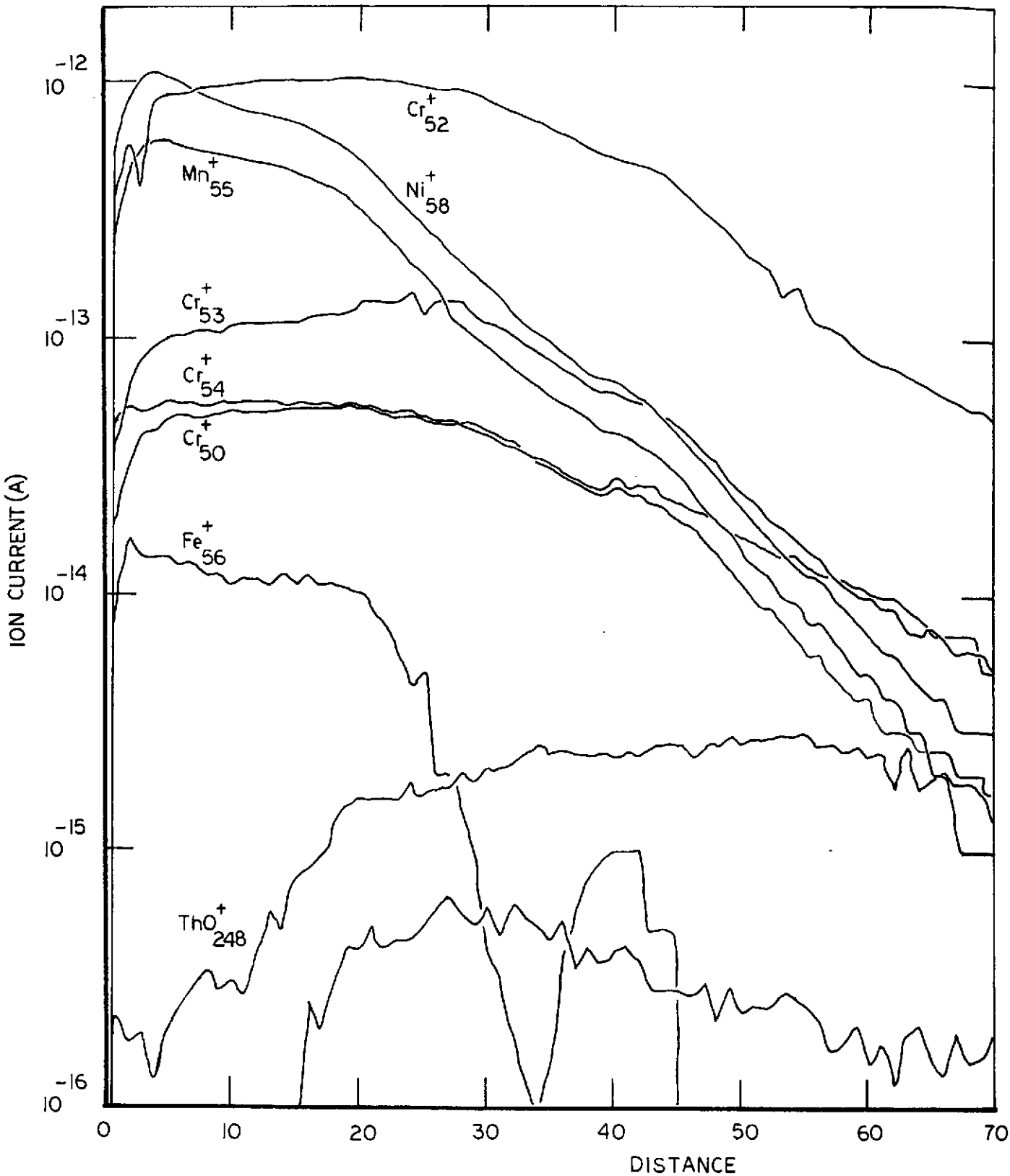

FIGURE 16d. CONCENTRATION PROFILE THROUGH OXIDE SCALE FORMED ON DSNiCrAl-Mn AFTER 6 x 10^2s (10 min.) AT 1473°K, (1200°C) 1.01 x 10^5 N/m^2 (760 torr) AIR (No. 65)

can be interpreted in the same way as Figure 16b, suggesting that in the manganese-doped alloy, the dopant is certainly present in an increased amount throughout the scale, yielding a signal some two orders of magnitude greater than that from the 0.05% Mn impurity in Figure 16b. No cobalt was detected in the cobalt-doped coupon (Figure 16c), but this is probably a result of the cobalt-containing outer layer of alloy having been removed in the pre-oxidation polishing.

Mechanical Testing

In order to determine the effect of the manganese dopant upon the mechanical properties of DSNiCrAl, room temperature tensile tests were made on coupons pack annealed in Batch 3 and oxidized under the same conditions as the standard oxidation coupons. The tensile test coupons were 0.0762 m (3 in.) long, by 0.0191 m (0.75 in.) wide on the shoulders, with a test section 0.0254 m (1 in.) by 0.0064 m (0.25 in.), and were cut with their length axis parallel to the rolling direction of the sheet.

As discussed previously, it was found necessary to remove a layer of adherent, thoria-free, pack-alloy from the surfaces of the doped coupons before oxidation testing in order to form adherent scales, so that it was decided to use standard oxidation coupons to generate the required oxidation data. The doped tensile test coupons were therefore oxidized with the as-pack annealed surface finish to avoid any possibility of non-uniform changes in test cross-section through surface grinding. Tensile test coupons of the undoped alloy were oxidized in the as-received condition, and the oxidation test data are listed in Table 11.

Tensile tests were made with an Instron Engineering Corp. machine operated at a strain rate of 0.005/min, and the 0.2% yield strengths, ultimate tensile strengths, and total elongations measured are given in Table 12.

It is immediately obvious that the DSNiCrAl alloy is considerably weakened after the pack annealing process, and that the manganese-doped alloy is weaker after oxidation, the UTS of the DSNiCrAl-Mn alloy being approximately 50% of that of the undoped alloy after pack annealing, and approximately 70% after oxidation. The difference after pack annealing might be explained by the formation of hard surface deposits high in aluminum, chromium, and manganese, as indicated in the concentration profiles measured through these coupons. It is difficult to reconcile the difference in strength after oxidation with the flat concentration profiles then existing in the coupons, and with a uniform concentration of 2% Mn. One possibility is that the increased aluminum content resulting from the pack annealing treatment is responsible for this change.

Also of interest is the slight tendency to an increase in strength after oxidation of the undoped alloy. It is thought that this might be the result of a change of the size, shape, or location of dispersed oxide particles in the alloy occurring by either internal oxidation or the solid-state conversion of chromia inclusions, for example, to alumina particles. Coupon No. 107 was oxidized for twice the exposure of the standard coupons at the higher oxygen pressure in an attempt to explore this effect, but appears to have become overaged.

TABLE 11. OXIDATION TEST DATA FOR TENSILE TEST COUPONS OF DSNiCrAl AND DSNiCrAl-Mn

Alloy	Specimen No.	Temp. °K	Temp. °C	Air Pressure N/m²	Air Pressure torr	Time* s	Time* h	Weight Change, kg/m²x10²	Remarks
DSNiCrAl	83	1373	1100	1.33×10^{3}	10	1.8×10^{5}	50	0.35	Little scale spallation
"	77	1373	1100	1.33×10^{3}	10	1.8×10^{5}	50,C	0.42	Little scale spallation
"	81	1373	1100	1.01×10^{5}	760	1.8×10^{5}	50	0.62	Specimen bent after oxidation, overgrowth of blue/green scale
"	79	1373	1100	1.01×10^{5}	760	3.6×10^{5}	(100,~ 53 cycles)	0.52	Slight scale spallation
"	73	1473	1200	1.33×10^{3}	10	2.12×10^{5}	59	0.62	Specimen bent after oxidation. Extensive scale spallation
"	85	1473	1200	1.33×10^{3}	10	2.84×10^{5}	(79,~ 55 cycles)	0.48	Specimen bent after oxidation
"	75	1473	1200	1.01×10^{5}	760	1.8×10^{5}	50	0.17	Specimen bent after oxidation. Extensive scale spallation
"	87	1473	1200	1.01×10^{5}	760	1.8×10^{5}	50,C	0.56	Specimen bent after oxidation, some scale spallation
"	107	1473	1200	1.01×10^{5}	760	3.6×10^{5}	100	0.66	Slight scale spallation
DSNiCrAl-Mn	82	1373	1100	1.33×10^{3}	10	1.8×10^{5}	50	-0.03	Extensive scale spallation
"	76	1373	1100	1.33×10^{3}	10	1.8×10^{5}	50,C	-0.10	Extensive scale spallation
"	80	1373	1100	1.01×10^{5}	760	1.8×10^{5}	50	0.01	Specimen slightly bent after oxidation. Extensive scale spallation
"	78	1373	1100	1.01×10^{5}	760	3.6×10^{5}	(100, ~53 cycles)	-0.17	Extensive scale spallation
"	72	1473	1200	1.33×10^{3}	10	2.12×10^{5}	59	-0.53	Extensive scale spallation
"	84	1473	1200	1.33×10^{3}	10	2.84×10^{5}	(79, ~55 cycles)	-0.03	Extensive scale spallation
"	74	1473	1200	1.01×10^{5}	760	1.8×10^{5}	50	-0.01	Extensive scale spallation
"	86	1473	1200	1.01×10^{5}	760	1.8×10^{5}	50,C	0.00	Specimen slightly bent after oxidation. Extensive scale spallation

* C = cycles of cyclic oxidation test.

1 cycle ≡ 1.8×10^{3} s at temperature

TABLE 12. TENSILE PROPERTIES OF DSNiCrAl ALLOYS.
UTS AND YS IN $N/m^2 \times 10^{-9}$

Condition		DS NiCrAl Spec. No.	UTS	0.2% YS	% EL	DS NiCrAl-Mn Spec. No.	UTS	0.2% YS	% EL
Before Oxidation		101, 102, 103	1041	793	7	100, 109	524	469	2
Isothermal, 1.8×10^5 s (50 h), 1.33×10^3 N/m^2 (10 torr) air	1373°K	83	1186	710	16	82	669	510	6
	1473°K	73	979	683	17	72	986	572	26
Isothermal, 1.8×10^5 s (50 h), 1.01×10^5 N/m^2 (760 torr) air	1373°K	81	841	786	11	80	731	552	7
	1473°K	75	1131	(614)	18	74	689	517	6
Cyclic, 1.8×10^5 s (50 h), 1.33×10^3 N/m^2 (10 torr) air	1373°K	77	1227	752	16	76	648	503	5
	1473°K	85	1110	696	15	84	758	676	5
Cyclic, 1.8×10^5 s (50 h), 1.01×10^5 N/m^2 (760 torr) air	1373°K	79	1186	717	21	78	634	593	2
	1473°K	87	1124	669	17	86	820	462	18
Isothermal, 3.6×10^5 s (100 h), 1.01×10^5 N/m^2 (760 torr) air	1473°K	107	1041	793	10	--	--	--	--

( ) = estimated value.

CONCLUSIONS

- The total normal emittance of DSNiCrAl can be increased to a maximum absolute value of 0.59 (at 1473°K) by the addition of 2-4% Mn. This is less than the value of 0.85 set as the goal for this program.

- This increased value of emittance is, however, within 85% of that measured for TDNiCr oxidized to form chromia scales, which was 0.69 (at 1473°K).

- The total normal emittance of DSNiCrAl can be increased to 0.67 (at 1473°K) if the alloy surface is highly-polished before oxidation. Such a surface treatment is probably not feasible in practice.

- The emittance change caused by Mn is thermally stable as judged by isothermal and cyclic oxidation tests for up to 1.8×10^5 s (50 h) in air at 1373 and 1473°K in 1.33×10^3 to 1.01×10^5 N/m^2 slowly-flowing air.

- The manganese-doped alloy exhibits only 50% of the UTS of undoped DSNiCrAl after the pack annealing treatment, but recovers to 70% of the UTS of the undoped alloy after oxidation.

- The pack annealing treatment results in an increase in the alloy aluminum content from 5.9% to almost 9.0% which may contribute to the change in strength.

- The manganese-doped alloy oxidizes at essentially the same rate as the undoped alloy, although a thin outer layer of transient scale containing $MnAl_2O_4$ is formed, and manganese is incorporated in the main alumina scale.

- Examination of the scales on the DSNiCrAl alloy suggest that thoria particles are incorporated throughout their thickness, and that growth occurs essentially at the metal/oxide interface. Some evaporation process, possibly of transient oxides, occurs from the outer surface of the scale.

- The observed scale morphologies and the distribution of the manganese in the scale are in general accord with current ideas of transient oxidation of such alloys.

- Thickness changes resulting from oxidation could not be measured for the surface-ground finished coupons used in this investigation.

ACKNOWLEDGEMENTS

Mr. R. O. Dodds performed a large part of the experimental work. Mr. C. L. Criner carried out the pack diffusion work, and Ms. M. R. Cantin was responsible for the tensile tests. Thanks are also due to Drs. A. H. Clauer and R. I. Jaffee for discussion and advice, and to D. F. Kohler, B. F. Phillips, J. F. Lagedrost, C. R. Barnes, and Mrs. D. Walnoha.

REFERENCES

1. C. E. Lowell, D. L. Deadmore, S. J. Grisaffe, and I. L. Drell, NASA TN D-6290 (1971).

2. F. J. Centolanzi, NASA TM X-62,015 (1971).

3. F. J. Centolanzi, H. B. Probst, C. E. Lowell, and N. B. Zimmerman, NASA TM X-62,092 (1971).

4. C. E. Lowell and W. A. Sanders, NASA TDN-6562 (1971).

5. M. S. Seltzer, B. A. Wilcox, and R. I. Jaffee, NASA Cr-120880 (1971).

6. Private communication with D. D. Briggs, Coors Porcelain Company (1972).

7. R. E. Taylor, Report to Metcut Research Associates, Inc., P.O. No. 54571, Task 2, March 20, 1972.

8. F. S. Pettit, Trans. Met. Soc. AIME, 239, 1296 (1967).

9. C. S. Giggins and F. S. Pettit, J. Electrochem. Soc., 118, 1782 (1971).

10. F. H. Stott and G. C. Wood, Corr. Sci., 11, 799 (1971).

11. B. H. Kear, F. S. Pettit, D. E. Fornwall, and L. P. Lemaire, Oxdtn. Metals, 3, 557 (1971).

12. C. R. Barnes, Met. Trans., 1, 1085 (1970).

13. C. W. Price, I. G. Wright, and G. R. Wallwork, Met. Trans., 4, 2423 (1973).

14. I. G. Wright and M. S. Seltzer, Met. Trans., 4, 411 (1973).

APPENDIX A

NEW TECHNOLOGY

NEW TECHNOLOGY

The research in this program has led to new technology in the area of increased emittance of protective alumina scales. This technology was the subject of a New Technology Report (G-1736-A) submitted to the Technology Utilization Officer, NASA-Lewis Research Center, on December 4, 1973.